A Late Pleistocene to Mid-Holocene Stable Oxygen Isotope Record from a Belize Stalagmite

Author: Maria Rose Crosby

Boston College Electronic Thesis or Dissertation, 2010

Boston College

The Graduate School of Arts and Sciences

Department of Geology and Geophysics

A LATE PLEISTOCENE TO MID-HOLOCENE STABLE OXYGEN ISOTOPE RECORD FROM A BELIZE STALAGMITE

a thesis

by

MARIA ROSE CROSBY

submitted in partial fulfillment of the requirements

for the degree of

Master of Science

September 2010

Abstract

A ~7,000 year stable isotope record from a Central American stalagmite is presented as a record of rainfall and consequently Intertropical Convergence Zone (ITCZ) tropical rain belt strength over the late Pleistocene to mid-Holocene. The “amount effect” explains the well-documented inverse relationship between rainfall amount and stable oxygen isotope values observed in tropical monsoon regions and consequently in stalagmite calcite from those regions. ITCZ rainfall influences much of the Central American tropical region and here a ~7,000 year stable isotope record from stalagmite ATM1 harvested from Actún Tunichil Muknal Cave in Belize is presented as a record of ITCZ influenced rainfall during the late Pleistocene to mid-Holocene (5,561 ± 2,488 BP - 12,605 ± 284 BP). Three major oxygen isotope excursions occur within the record. These excursions correspond to the global cold Younger Dryas and 8.2 ka events and a relatively undocumented wet period around 6,300 bp. The Younger Dryas manifests as a relatively moist period in central Belize while the 8.2 ka event manifests as a relatively dry period. The reason for the opposite responses to cooling elsewhere in the globe is posited to be due to orbital forcings. The 6,300 bp relatively wet period appears to be synoptic in scale and two possible triggers for the isotope excursion are presented: eustatic sea level rise causing lagoonal constriction, warming of water off the coast of Belize, and thus increased evaporation and precipitation over the study region; and hurricane clusters, evidenced in the region in the succeeding 1,000 years, in which the location of the Azores High funnels hurricanes to make landfall near the central Belize region.

ATM1 provides evidence for tropical leads and/or lags to global climate events and bolsters the idea that high and low latitude climate relationships are complexly interlinked.

Table of Contents

List of Figures

List of Tables

List of Appendices

Introduction

Climate during the last deglaciation (late Pleistocene) and Holocene epoch is of great interest today because of its potential for use as an analog for current rapidly changing global climate conditions (Hughen et al., 1996). Tropical climate is especially of interest because of the role it plays in global heat transfer (Lachinet et al., 2004). ITCZ (Intertropical Convergence Zone) rainfall influences much of the Central American tropical region and here a ~7,000 year stable isotope record from stalagmite ATM1 harvested from Actún Tunichil Muknal Cave in Belize (Figure 1) is presented as a record

Figure 1. Cave locality from which ATM1 was harvested, Actún Tunichil Muknal cave, Belize (star). (base map from Google Earth)

of ITCZ influenced rainfall during the late Pleistocene to mid-Holocene (12,605 ± 284 BP - 5,561 ± 2,488 BP).

Speleothems, or cave formations, retain clues to the long-term rainfall record in the form of stable isotope ratios contained in calcite (c.f. Gascoyne 1992). Tropical rainfall percolating through soil increases in partial pressure of CO_2 (PCO_2) due to high PCO_2 in the soil; high CO_2 in the soil is a result of decomposition of organic matter. This increase in PCO_2 of the infiltrating rainwater (vadose zone groundwater) makes it more acidic, and subsequently when infiltrating through limestone bedrock, it dissolves calcite. The groundwater becomes supersaturated with respect to calcite and when it reaches the cave atmosphere it begins to degas until equilibrium with the cave atmosphere PCO_2 is reached. This quick degassing of dissolved CO2 leads to a supersaturation of calcium carbonate and a precipitation of calcite from the drip water onto a stalagmite or other surface in the cave (Hendy 1971). Speleothems are good candidates for long-term rainfall records because they grow in sheltered environments and have been dated as far back as 350,000 years before present (McDermott 2004).

The “amount effect” describes the inverse relationship between stable oxygen isotope values and rainfall amounts in the tropics (Dansgaard 1964, Rozanski et al. 1993). The validity of the “amount effect” in the Belize region affected by ITCZ rainfall is demonstrated by monthly rainfall stable oxygen isotope averages during the N hemisphere wet season (Jun-Mar) having a lower mean value than those in the N hemisphere dry season (Mar-May). In Veracruz, Mexico (average annual rainfall = 1,574 mm/year, compared to the cave site’s 1,475 mm/year), the closest location to the cave site with an International Atomic Energy Agency [IAEA] precipitation isotope monitoring station, stable oxygen isotope values ($\delta^{18}O$) show an ~4 ‰ decrease during the wet season (International Atomic Energy Agency 2009) (See Appendix A for information regarding stable isotope notation). Wet season rainfall average $\delta^{18}O$ values are ~5 ‰, and dry season averages are ~1 ‰. Belize has a water deficit from early March through late May and experiences monsoon rainfall during the summer (Figure 2). Many mechanisms have been proposed to explain this phenomenon (Daansgaard 1964), but the fact remains that the amount effect dominates the $\delta^{18}O$ values in the Belize region (Lachinet and Patterson 2009).

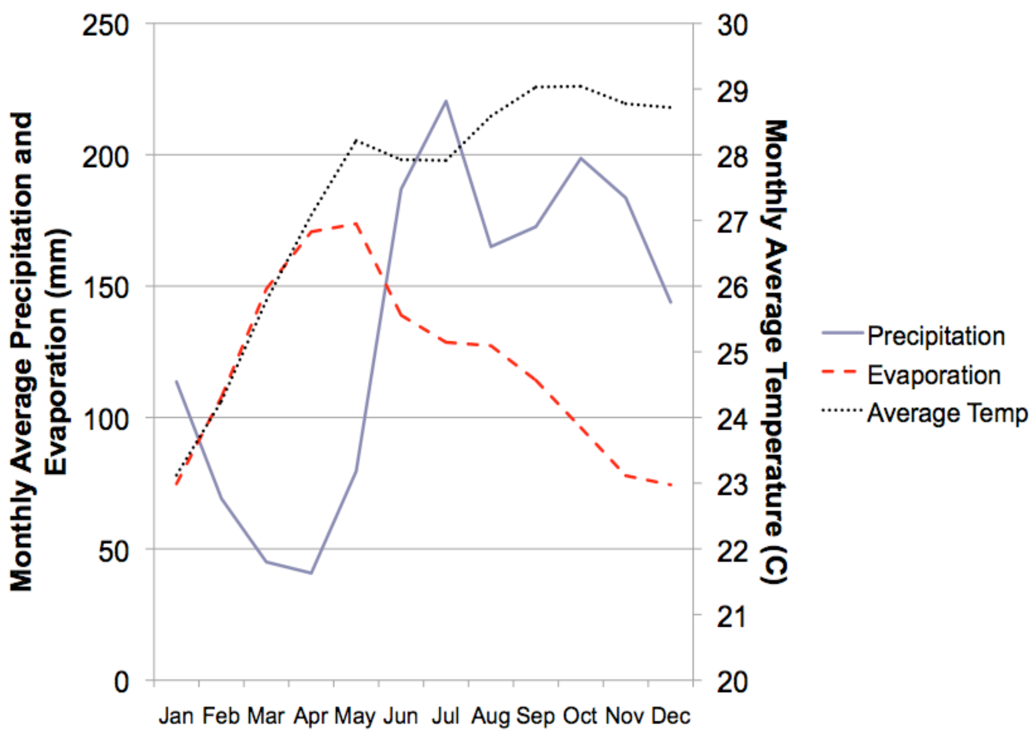

Figure 2. Central Farm, Belize climate data. Precipitation, evaporation and monthly average temperature averaged from 1966-2006 from the Central Farm meteorological station in Belize. The station is located less than 15 km from cave site.

Because of the inverse relationship between rainfall and stable oxygen isotope values, and because stalagmite isotope records are known to be useful archives for the paleo-rainfall signal (Gascoyne 1992, Nott 2004), stalagmites are the archive of choice for this study.

The retention of the rainfall stable isotope signature in cave formations is dependent on both the extent of dilution of storm water by groundwater as it flows through the epikarst, and supersaturation of infiltrating water with respect to calcite (Frappier et al. 2007). The cave depth is an important control on signal preservation as well. If the cave is too shallow and infiltration time is short, it is unlikely the drip water will be supersaturated with respect to calcite, and no deposition (and possibly erosion) will occur. Alternatively, if the cave is too deep, the rainfall signal of any individual storm event is likely to be homogenized with the ground water and only persistent, long-term climate signals will be preserved (Frappier et al. 2007).

Many factors could confound the direct rainfall oxygen stable isotope signal, however as posited here, none are expected to affect the isotope record significantly. The absence of kinetic isotope effects (known as isotopic equilibrium) is also important in climatic signal preservation in speleothem isotope records (Dorale et al. 2002). Isotopic equilibrium deposition conditions are usually necessary for preservation of the rainfall signal, because kinetic fractionation occurring on stalagmite surfaces at the time of deposition masks the rainfall signal carried by the drip water (Dorale et al. 2002). The conditions of isotopic equilibrium are slow degassing rates, and no evaporation; fractionation between the aqueous and solid phases must be dependent on only temperature (Hendy 1971). Under isotopic equilibrium conditions, environmental inputs produce the primary signal recorded through isotope ratios (Dorale et al. 2002).

High relative humidity in the cave (>95%) is expected to minimize the effect of partial evaporation of drip water while on the surface of the stalagmite. Cave temperature remains relatively constant, with the average temperature reflecting the mean annual temperature above the cave; thus the effect of fractionation at different temperatures is eliminated because of stable cave atmosphere temperatures (Kim and O'Neil 1997).

Oxygen in cave drip water is sourced primarily from rainfall above the cave, with a minor contribution from carbonate ions produced by bedrock dissolution and dissolved soil carbon dioxide (Richards and Dorale 2003). This meteoric drip water infiltrates the epikarst (bedrock above the cave) and is in turn incorporated into speleothem calcite. The climate signal recorded in speleothems is primarily controlled by the isotopic composition of rainfall (McDermott 2004). Speleothems can record rainfall on timescales of years to millennia (Burns et al. 2001). Therefore, the stable oxygen isotope record from ATM1 is interpreted here as a rainfall proxy. Each stable isotope sample in the ATM1 record averages a 35 yr span of calcite deposition. Therefore, it is possible to use this record for analysis of climatic changes on centennial to millennial timescales with lower $\delta^{18}O$ values indicating wetter conditions, and vice versa.

Global climate events during the Late Pleistocene to Mid-Holocene, such as the Younger Dryas, and the 8.2 ka event, have been studied at many locations (Lachinet et al., 2004; Denniston et al., 2001; Leyden, 1995) however, few studies have determined the temporal relationship between these high latitude events and the tropics in terms of lead or lag relationship. Hughen et al. (1996) discuss the role of North Atlantic sea surface temperature changes in tropical North Atlantic trade wind strength during the last glaciation until about 8,000 bp while Cai et al. (2010) found that in the Central China monsoon region shifts in monsoon strength from 4,500 bp to 7,500 bp occurred from south to north. The record presented here from the ATM1 stalagmite seeks to elucidate the role and response of Central American ITCZ rainfall with regard to major high latitude climate events over the late Pleistocene to mid-Holocene.

Methods

ATM1 (Figure 3) was collected from Actún Tunichil Muknal cave (Figure 1) in Belize by Amy Frappier and her team in January 2001 using a sampling approach outlined in Frappier (2006). The stalagmite was halved and polished along the longitudinal growth axis by Amy Frappier. Maria Crosby while visiting the University of

Figure 3. ATM1, 32.25 cm stalagmite from Actún Tunichil Muknal Cave, Belize.

Minnesota conducted radiometric dating sample collection. Xianfeng Wang at the University of Minnesota completed U/Th radiometric dating. Stable isotope micromilling samples of the top 2.7 cm along the growth axis were collected by Maria Crosby at Woods Hole Oceanographic Institute and the stable isotope data analysis was conducted by Dorinda Ostermann at Woods Hole Oceanographic Institute. The following subsections describe this study's paleoclimate archive material , stalagmite ATM1, as well as the methods used herein for dating and stable isotope analysis.

ATM1

ATM1 (Figure 3), a 32.25 cm long stalagmite from Actún Tunichil Muknal cave (17° 11′ 23.56″ N, 88° 29′ 51.54″ W) in central Belize (Figure 1) was harvested on January 10, 2001 by Amy Frappier and her field assistant as part of an effort to collect hurricane-sensitive stalagmites (Frappier et al. 2007). The topmost section, 8.2 cm long, was used in this study. ATM1 was collected in the 'Two Babies Room' of the cave and was growing on the side of a column with multiple attachment points to the wall. The room was 25°C and had a relative humidity of over 95-100% at the time of collection. The wet top of the stalagmite was off-white while the rest of the stalagmite was the same reddish-brown color as the fine cave mud in the area. The stalagmite was fracture-fed, and the source water came from a soda straw 40 cm above. ATM1 has a 'broomstick' shape, and field notes indicate another 2+meter long broomstick-shaped stalagmite in this room of the cave. The existence of the two similar stalagmites in the room indicates quiet depositional conditions persisted in this part of the cave for a long period time. Drips were observed to fall onto the top of ATM1 relatively slowly, at intervals of a few minutes (Frappier, 2000-2001 field notes). ATM1 was cut in half along the vertical growth axis using a diamond blade circular saw and polished by Amy Frappier. The stalagmite section used in this study was mounted in epoxy, polished side up, to stabilize and keep it level during stable isotope sample collection. X-ray diffraction conducted at University of Iowa confirmed the sample was made of pure calcite (Frappier 2002).

Dating

^{238}U-^{234}U-^{230}Th radiometric dating was used to create an age model for ATM1. Lack of demonstrable annual layers prohibited the constraint of ages at greater resolution than layers sampled and dated by U/Th methods.

Radiometric Dating

^{238}U-^{234}U-^{230}Th radiometric dating was conducted at the University of Minnesota. Powdered samples were drilled in clear white calcite at 2.4-4.6 mm, 10.2-12.6 mm, and 14.6-16.6 mm from the top (Figure 4). Effort was made to draw each sample from the fewest number of visible laminae possible in order to minimize the span of time accounted for in each sample. The samples were drilled using a foot pedal-controlled dental drill with a 0.9 mm carbide drill bit. The drilling was completed in a laminar flow fume hood and the drill bit was dipped in HNO_3 and ethanol after each sample was taken in order to prevent cross contamination. The samples, ranging in weight from 0.1 g to 0.2 g, were collected on weighing paper, weighed and transferred to glass vials. The samples were prepared for analysis by Xianfeng Wang and analyzed using the Thermo-Finnigan Neptune ICP-MS (Inductively Coupled Plasma Mass Spectrometer) at the University of Minnesota. Sample ages in calendar years were computed following standard method (Shen et al., 2002). Linear interpolation between dated intervals was then used to create an age model as described below. All dates are reported as years before 2007.

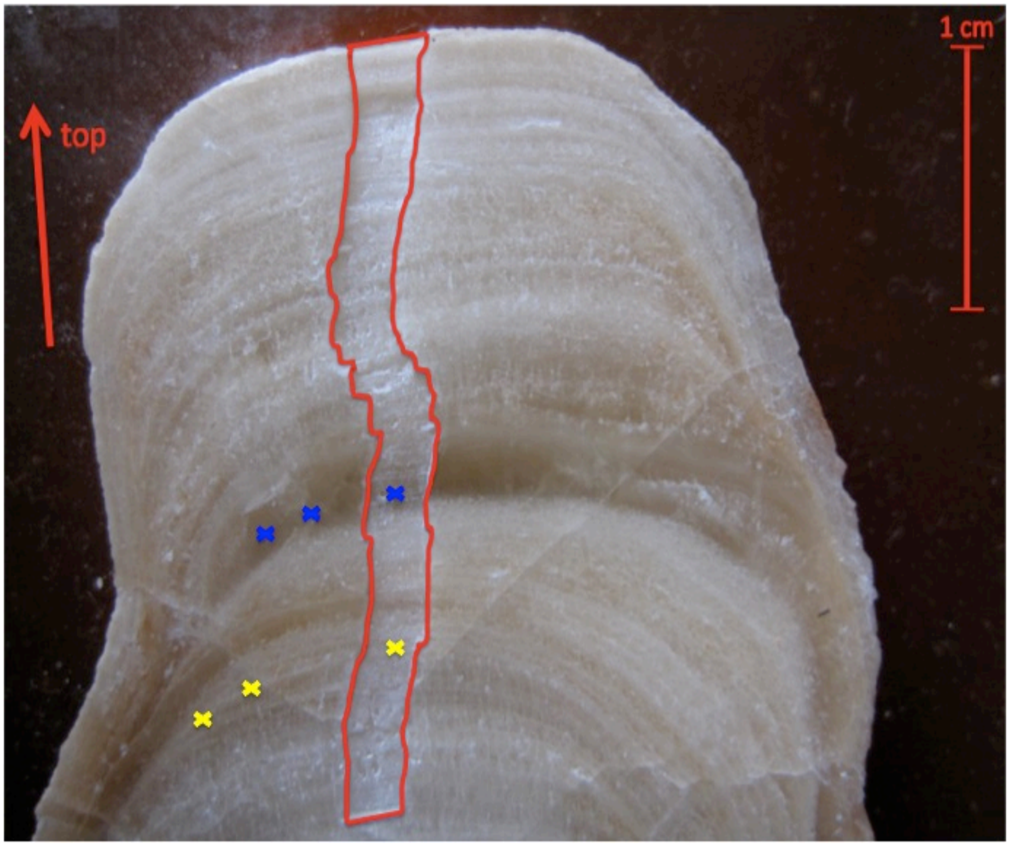

Figure 4. Top-most portion of ATM1. Red outlines the track along which micromilled samples were taken. Blue Xs indicate Hendy Test 1 sample points, and yellow Xs indicate Hendy Test 2 sample points. U/Th radiometric dates taken from other half of stalagmite at 2.4-4.6 mm, 10.2-12.6 mm, and 14.6-16.6 mm down from top of ATM1.

Age Model

The age model for ATM1 is created based on radiometric dates obtained from samples drilled at the University of Minnesota. The U/Th dating procedure assumes that initial Th is negligible, and thus all Th detected in a sample is radiogenic (Shen et al., 2002). This assumption is generally valid because U is soluble in water, while Th is not; water from which the stalagmite calcite is precipitated therefore would contain some U and no Th. Stalagmites stay closed systems after calcite has precipitated, and thus all Th detected during the dating process is assumed radiogenic (Shen et al., 2002). However, it is possible that initial Th concentrations in ATM1 were not negligible and may have interfered with the calculation of accurate dates. Higher amounts of Th in the sample are assumed to mean that more time has passed since the time of deposition. However, if initial amounts of Th were higher than assumed, the date would overestimate the true age of the sample. There is no way to calculate the true initial Th concentrations without having a sample of the water from which the stalagmite calcite was precipitated.

U/Th dating samples for ATM1 were taken at depths of 2.4-4.6 mm, 10.2-12.6 mm, 14.6-16.6 mm. Amy Frappier collected ATM1 and her field notes indicate that the top was wet at the time of collection indicating active growth, thus making the top of the stalagmite of modern age. Stalagmite stratigraphy dictates that age must increase with depth. The top two dates (from 2.4-4.6 mm and 10.2-12.6 mm) show a decrease in age with depth, and thus a dating error must have occurred with one or both samples.

Stable Isotope Analysis

Calcite powder samples were micromilled for Hendy tests of equilibrium calcite deposition along layers at depths of 1.64 cm and 2.45 cm. Powder samples were also collected continuously at 20 μm intervals along the top 2.7 cm of the growth axis for stable isotope analysis.

Hendy Test for Equilibrium Calcite Deposition

Equilibrium calcite deposition conditions ensure the climatic stable isotope signal is the primary control on stable isotope values in the calcite (Lauritzen and Onac 1999).

A test for equilibrium deposition conditions developed by Hendy (1971) examines the influence of equilibrium fractionation versus kinetic processes on calcite deposition along a single growth layer. If kinetic effects (i.e. disequilibrium processes) dominate, then stable oxygen isotope values in the calcite of a single growth layer will change > 0.8 ‰ (Gascoyne 1992) with distance from the growth axis; with equilibrium conditions, no significant changes in $\delta^{18}O$ values will be observed. Carbon stable isotopes are expected to increase with distance from the growth axis (due to outgassing) in both equilibrium and kinetic dominated deposition; thus covariation of carbon and oxygen stable isotopes is not expected during equilibrium deposition.

The “Hendy Test” was performed on two separate bands/growth layers in ATM1 (Figure 4) at depths of 1.64 cm and 2.44 cm. Three samples were taken along a growth layer for each test including the sample from the growth axis. The vertical portion of the growth layer (along the sides of the stalagmite) could not be sampled, as reliable identification of the growth layers was not possible.

Micromilling

Micromilled samples were collected continuously at 20 μm intervals along the growth axis of ATM1 using a Merchantek computerized microdrill at Woods Hole Oceanographic Institute (WHOI). A total of 1,328 samples were collected along the ~2.7 cm transect. Sample weights ranged from 20 μg to 70 μg with mean weight of 42 μg. The depth interval of each sample location was 0.5 mm, and each sample was drilled using 5 passes of the drill bit. The depth per pass was 100 μm. Each sample was drilled from a 2.5 mm wide section of the stalagmite (red track in Figure 4).

A transect was defined along the polished cross-sectional surface of the stalagmite where drilling was to take place using the microscope view of the drill, characteristics of the micro-sample collection procedure (described above) were set and a stream of compressed air was then used to clean off the drill and stalagmite surface before the drill was set to work. A clean steel micro spatula was used to collect the powder from the stalagmite surface and transfer it to a tared sample boat. The micro-sample was then weighed, its weight recorded and transferred from the stainless steel sample boat to a vial which was to be placed directly in the mass spectrometer.

The 1,328 calcite powder samples from ATM-1 were analyzed using a Kiel III carbonate device coupled to a Finnigan MAT 253 mass spectrometer at Woods Hole Oceanographic Institute (WHOI), under the direction of Senior Scientist Simon Thorrold and Lab Director Dorinda Ostermann. All ATM-1 stable isotope values are reported in per mil (‰) relative to V-PDB (See Appendix A for an explanation of stable isotope notation). Raw data was filtered using guidelines provided by the lab at WHOI. Out of the 1,328 samples 1,266 produced useful data. Sixteen of the samples were lost due to user error; seven did not contain enough material (< 20 μg) to produce dependable results; twelve did not have sufficient voltage (< 0.6 volts). For twelve samples, the degree of balancing between the standard voltage and the sample voltage was too great (>2.5 volts); and twelve had more than 4 outliers (meaning the machine could not determine which of the 8 scans was unreliable and mean values were not calculated accurately); 66 total samples were discarded and not used for study analysis. The remaining 1,266 data points spanned the ~2.7 cm transect and 201 samples spanned the reliably dated section from 1.14 cm to 1.56 cm. The focus of the study is on the 201-micromilled stable isotope samples from this section. The stable isotope data from above and below this section presented below are available for further studies after additional reliable dates are obtained and a more complete age model is developed.

Results

Radiometric dating and linear interpolation were used to create an age model for ATM1. A 1,266-sample assay of stable carbon and oxygen isotope composition of the stalagmite calcite was compiled from a 2.5 mm wide track along 2.7 mm of the growth axis. Because only two radiometric dates are reliable, the results present only the 201 stable isotope data points corresponding to the dated section of ATM1.

Dating

Radiometric dating was used as the basis of the ATM1 age model. A study of the stratigraphy shows visible and fluorescent banding, none at a frequency that corresponds to annual layering verifiable by the radiometric data available. Because only two dates are viable, the age model for this study is constrained between 5,561 bp ± 2,488, and 12,605 bp ± 284.

Radiometric Dating

The three U/Th dates taken at depths of 2.4-4.6 mm, 10.2-12.6 mm and 14.6-16.6 mm yielded dates of 8,533 bp ± 1,367, 5,561 bp ± 2,488, and 12,605 bp ± 284 respectively (Table 1). Because age must increase with depth, there must be a dating error in one of the top two dates. When dates are stratigraphically inconsistent, at least one of them is likely to be unreliable and incorrect.

U/Th radiometric dating is based on the assumption that initial Th content in the calcite sample is low to negligible. This assumption is violated in the top-most dating

Sample	Depth	Weight	^{238}U	^{232}Th	$\delta^{234}U$	$[^{230}Th/^{238}U]$	$[^{230}Th/^{232}Th]$	Age
	(mm)	(g)	(ppb)	(ppt)	measured	activity	(ppm)	(years before 2007)
ATM1-T	3.5	0.21	19.4 ± 0.1	3605 ± 11	1080.0 ± 9.8	0.20313 ± 0.00665	18 ± 1	8,533 ± 1367
ATM1-M	11.4	0.12	18.8 ± 0.1	1847 ± 15	1048.2 ± 9.6	0.12732 ± 0.04298	21 ± 7	5,561 ± 2488
ATM1-B	15.6	0.13	38.9 ± 0.1	38 ± 5	993.4 ± 6.0	0.21994 ± 0.00466	3740 ± 550	12,605 ± 284

Table 1. U/Th data for the three samples taken for radiometric dating from ATM1.

sample (and stratigraphically youngest) from ATM-1 and thus makes the date suspect. ^{230}Th contamination makes the calculated U/Th age of a sample too old, and this is seen in the top U/Th date of ATM-1. The other U/Th radiometric samples have a lower initial thorium content, and are thus more reliable; thus, the top-most radiometric date from ATM-1 will be discarded and the bottom two dates will be used in this study. High initial Th content in stalagmite calcite may arise from volcanic fall out.

It is proposed that fallout from the 1982 El Chichón volcanic eruption caused high initial Th concentrations in the top date (2.4-4.6 mm depth) from ATM1. It is plausible that the sample taken 2.4-4.6 mm from the top for U/Th dating included calcite deposited directly after the 1982 eruption, which likely contained elevated Th concentrations. Actún Tunichil Muknal cave is known to have been dusted with ash from the 1982 El Chichón eruption. An independently dated stalagmite from the same cave, stalagmite ATM7, was analyzed for trace elements in a previous study (Frappier 2002). This analysis yielded an increase in Th concentrations of 7-9 orders of magnitude above background levels over the 0.6 mm section of ATM-7 following the date of the eruption. U concentrations increased 3 orders of magnitude over the same section. Therefore, it is likely ATM1 was also an archive for the eruption products. Because of the nature of the ash, initial Th in the dating sample was likely not negligible, violating the assumption of

U/Th dating that initial Th concentrations are either zero or constant and known, indicating U/Th dating methods were confounded by the presence of initial Th in the system. Thus, the date from 2.4-4.6 mm is deemed unreliable. The potential influence of the eruption, and the age of the sample being older than the one stratigraphically below it deem this date unreliable and it will not be used in this study. While the 2.4-4.6 mm U/Th date is suspect, there is no known evidence to suspect that Th from volcanic ash or any other source contaminated the lower U/Th dating samples, and thus the remaining two dates are thought to be reliable.

Age Model

The dates that will be used in this study come from 10.2-12.6 mm and 15.6 mm from the top of the stalagmite growth axis, and yielded dates of 5,561 ± 2,488 and 12,605 ±284 years before present. This time interval spanning the late Pleistocene and early to mid-Holocene is the focus of this study. Lack of annual layering over the growth interval prevents further constraint of ages. With no other information available, simple linear interpolation is used to create an age model for ATM1 (Figure 5).

The linear growth rate of ATM1 between 5,561-12,605 years before present is approximately 6.0×10^{-4} mm/yr for the 7,044 yr study period. Although a linear growth rate may not be plausible over epochs, it is the best assumption for the dates obtained. Each stable isotope micromilled sample represents approximately 35 years.

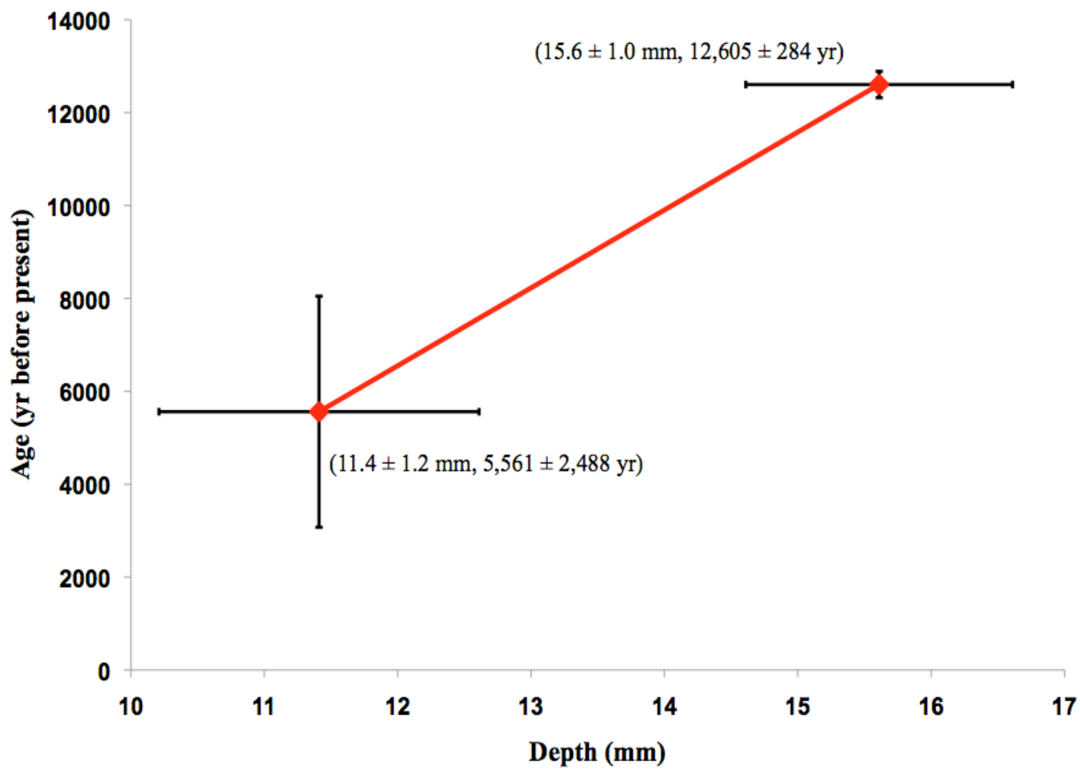

Figure 5. ATM1 age model. Linear interpolation used between viable U/Th dates to create age model (red line). Growth rate is approximately 6.0 x 10^{-4} mm/yr for the 7,044 yr study period.

<u>Micromilling Data</u>

Micromilled stable isotope data for carbon and oxygen in ATM1 is deemed reliable because of evidence indicating equilibrium deposition conditions.

Test for Equilibrium Calcite Deposition

Two Hendy tests for equilibrium calcite deposition were conducted, one at 1.64 cm depth and one at 2.44 cm depth. Each test included the data from the growth axis and two additional sample points along the same growth layer. The right-hand column in

Figure 6 shows a bivariate plot for carbon and oxygen stable isotopes. In the “Hendy 1” band, covariation between carbon and oxygen does exist; in the band “Hendy 2” there is no significant covariation between the stable isotope values. The covariation in carbon and oxygen isotopes in band 1 may indicate disequilibrium deposition, however it might intested be an artifact of the data having too few sample points to determine a true covariation. Because oxygen isotopes in the growth layer behave as expected in equilibrium dominated deposition, and because sampling was done at the growth axis where equilibrium processes are most likely to dominate, it is assumed for the purposes of this study that ATM1 calcite was deposited in equilibrium with drip water; both bands pass the Hendy test for equilibrium deposition.

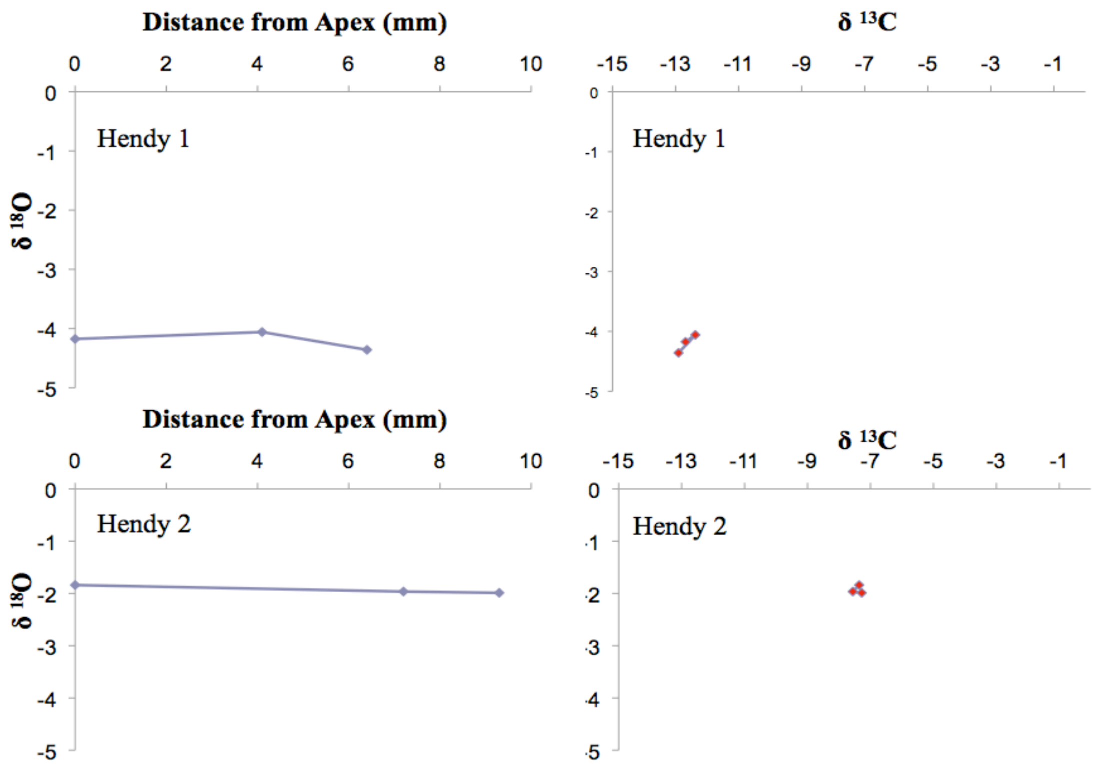

Figure 6. ATM1 Hendy Test Results. Hendy 1 was taken from 1.64 cm depth and Hendy 2 was taken from 2.44 cm depth. Both bands pass Hendy Test.

Stable Isotope Data

Through the 2.7 cm micromilled transect, the oxygen stable isotope values (Figure 7) during the study period are the highest of the post-Pleistocene record reaching a maximum of -2.285‰ at 13.15 mm depth. The carbon stable isotope values during the study period represent an increase from previous levels followed by a return to pre-study period levels at the end of the study interval. Compared to ATM7, a stalagmite from the same cave with a modern record of climate, oxygen stable isotope values are higher in ATM1 indicating an overall drier climate than modern times. The ATM7 record has an

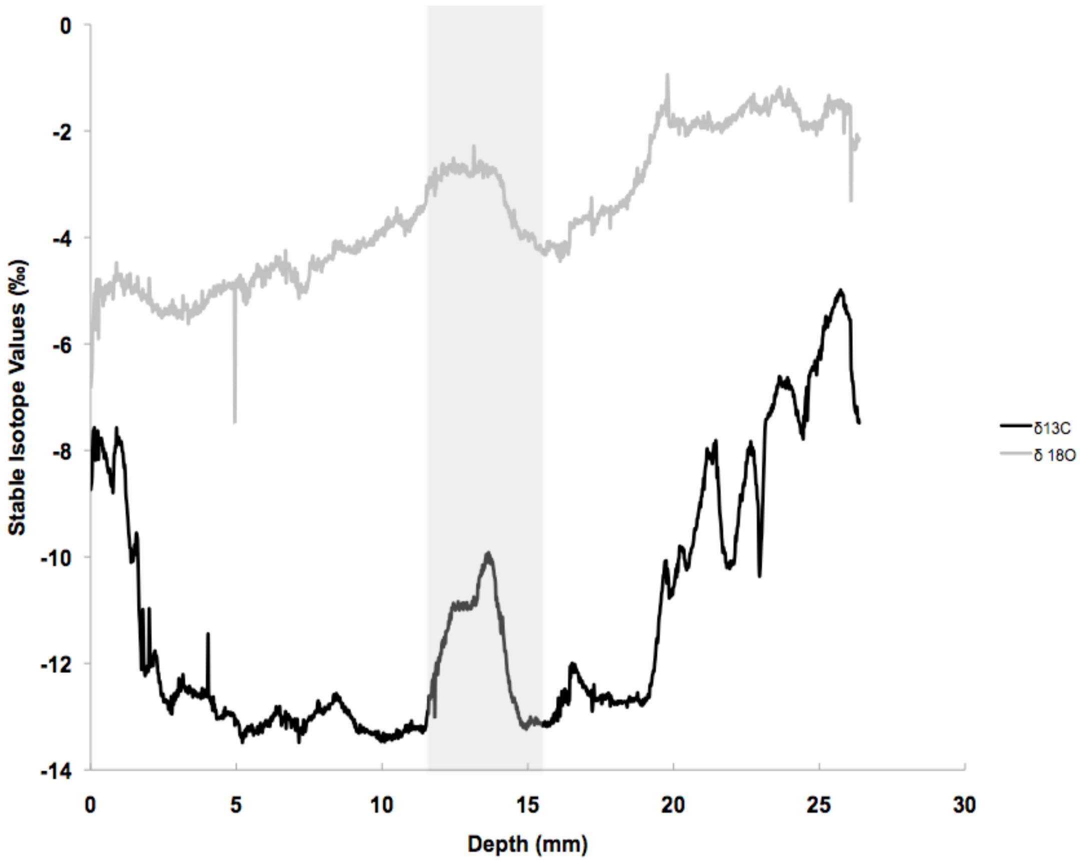

Figure 7. Stable isotope values from ATM1. Carbon and oxygen stable isotope values obtained from micromilling transect along 2.7 cm of growth axis of ATM1. Shaded area indicates interval focused on in this study.

average stable oxygen isotope value of -3.745‰ while the ATM1 study period record has an average of -2.987‰.

Oxygen stable isotope values during 5,561 – 12,605 bp (Figure 8) ranged from -4.326‰ to -2.285‰. The mean value is -3.165‰ and the standard deviation is 0.555. The maximum of -2.285‰ occurred 8,554 bp, and the minimum of -4.326‰ occurred 12,534 bp. The largest positive excursion is 0.39‰ and occurred between 8,589 and 8,554 bp. The largest negative excursion (-0.43‰) occurred between 6,195-6,300 bp.

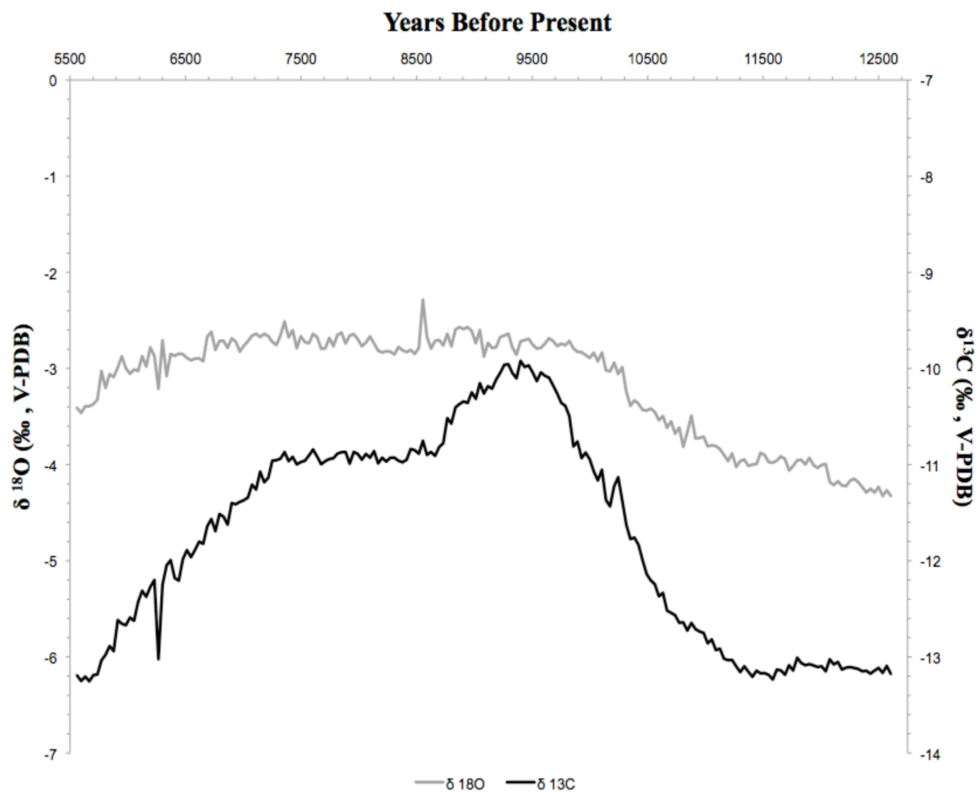

Figure 8. **ATM1 carbon and oxygen stable isotope time series (5,500-12,500 bp). δ ^{18}O values steadily increase until approximately 9.780 bp when there is a general leveling off of values. δ^{13}C values generally increase until 9,399 bp after which they decline until 8,589 bp and 7,322 bp values level off; between 7,322 and 5,561 bp values generally decline.**

Because the dataset spans two epochs, each epoch's array was evaluated independently; from 12,605-~9,700 bp δ^{18}O values increase, then level off until 5,561 bp. Holocene δ ^{18}O data (5,561-11,477 bp) (onset of Holocene as defined by U.S. Geological Survey 2007) has a mean of -2.987‰ and a standard deviation of 0.405‰ while the late Pleistocene portion of the data set (11,477-12,605 bp) has a mean of -4.104‰ and a standard deviation of 0.139‰. This 1.117‰ difference in oxygen stable isotope ratios from consecutive epochs is significant within a dataset with a total range of 2.041‰.

$\delta^{18}O$ values steadily increase until approximately 9,700 bp when there is a general leveling off of values.

Autocorrelation spectral analysis, which determines the significant frequencies of a time series, detected no significant periods (frequencies) within the $\delta^{18}O$ record in either epoch segment.

Carbon stable isotope values from 5,561-12,605 bp (Figure 8) have a range of 3.333‰ between -13.254‰ and -9.921‰. The mean is -11.752‰ and the standard deviation is 1.084. The maximum value (-9.921‰) occurred 9,399 bp and the minimum value (-13.254‰) occurred 5,666 bp. The largest positive excursion occurred between 10,351 and 10,140 bp with a magnitude of 0.21‰ while the largest negative excursion occurred between 6,300 and 6,195 bp and has a magnitude of -0.77‰.

Holocene $\delta^{13}C$ values have a mean of -11.492‰ and a standard deviation of 0.987‰. Pleistocene $\delta^{13}C$ values have a mean of -13.121‰ and a standard deviation of 0.049. $\delta^{13}C$ values generally increase until 9,399 bp after which they decline until 8,589 bp. Between 8,589 bp and 7,322 bp values level off; between 7,322 and 5,561 bp values generally decline. Autocorrelation spectral analysis detected no significant periods (frequencies) within the $\delta^{13}C$ record or either epoch segment.

$\delta^{18}O$ and $\delta^{13}C$ values are positively correlated and have a R^2 value of 0.73. Near the lowest $\delta^{13}C$ values there is a divergence from this trend where $\delta^{13}C$ values stay relatively steady while $\delta^{18}O$ values change.

Discussion

Stable isotopes are a common paleoclimatic tool used to extract information about past climate conditions in many parts of the world. There are many different archives of stable carbon and oxygen isotope data including glacial ice (ex. Alley 1993) and stalagmite calcite. This study compares the timing of paleoclimatic events interpreted from glacial ice, lacustrine, bog, lagoon and atoll sediments, with the ATM1 records with the goal of determining the presence of global climatic events over Actun Tunichil Muknal cave in central Belize.

The limits of this study force the assumption that there is a linear growth rate across epochs. This assumption is not likely to reflect real conditions in this study area, especially in light of evidence that tropical climatic conditions were variable through the study period (Cai et al, 2010; Lachinet et al., 2004, Hughen et al., 1996). Climatic changes (i.e. amounts of rainfall in Belize) influence the residence time of water in the cave overburden and therefore affect the drip rate and consequently growth rate. Further dating methods must be employed in future studies if more realistic conclusions are to be drawn from ATM1 data. Nevertheless, working from the constraints of the best available linear growth model presented above, the present study compares ATM1 stable isotope data from the late Pleistocene and early to mid Holocene with other paleoclimatic archives to examine the tropical response to global climate events such as the Younger Dryas, the 8.2 ka event and the 6,000 bp event.

Holocene vs. Pleistocene Record

Holocene and Pleistocene portions of the oxygen stable isotope record have a

1.117‰ difference in mean values, with Pleistocene values having a mean of -4.104‰ and Holocene portions of the dataset having a mean of -2.987‰. There is an abrupt increase in both stable oxygen and carbon isotope values around 10,300 bp. The $\delta^{18}O$ record indicates wetter conditions (via the "amount effect" [Dansgaard 1964]) in the Yucatan Peninsula during the last glaciation as compared to the early Holocene.

This relatively wet period is also recorded in Lake Quexil, Guatemala fossil records (Leyden 1996). The Lake Quexil records indicate a cooling of 1.5 ºC and a persistence of high-moisture conditions between 12,000 bp and 10,300 bp. Increasing precipitation during this time may have been caused by the increasing of seasonality concurrent with this period (Berger 1978). This increasing seasonality caused an increase in monsoonal activity by affecting the annual movement of the inter-tropical convergence zone. A consistent monsoon climate may have protected the Belize region from colder temperatures prevailing elsewhere on the planet during the late Pleistocene (Leyden 1995).

Climatic Events Recorded in ATM1

The 7,000-year ATM1 record spans several short, global climatic events. The abrupt climate change events focused on in this project include The Younger Dryas, the 8.2 ka event, and a warming event that occurred ~6,000 bp.

The Younger Dryas

The Younger Dryas, a 1,300-year long cold period lasting from 12,800-11,500 bp, is recorded in several climate archives. Most records are from the Northern Hemisphere, although there is evidence of the event in the Southern Hemisphere (Cruz et al. 2006). This late Pleistocene event is characterized by an abrupt onset and termination, and temperatures in Greenland ~15 ºC colder than today (Alley 1993). The prevailing theory is that the draining of major glacial lakes during deglaciation caused the Younger Dryas. The freshwater pulse from glacial Lake Agassiz, in particular, caused a shutdown of thermohaline circulation and a reduction in heat transport towards the poles. This caused a resurgence of glaciers in the northern hemisphere, and cooler temperatures worldwide (Alley 2000).

Though the ATM1 record in this study spans part of the Younger Dryas stadial, it does not include pre-Younger Dryas paleoclimate information. This prohibits comparison of pre- and peri-conditions; it is not possible to determine whether the climate in the Yucatan during the period coincident with the Younger Dryas is a continuation of prevailing climate conditions at the time or associated with the Younger Dryas stadial. The record does, however, span the end of the Younger Dryas event. The termination of the event, around 11,500 bp, is coincident with the beginning of an increasing trend in ATM1 $\delta^{18}O$ and $\delta^{13}C$ values that lasts 800 years for oxygen (until 10,300 bp) and 2,200 years for carbon (until 9,300 bp). $\delta^{18}O$ values level off during the Holocene while $\delta^{13}C$ values decrease. Because of possible variable growth rates through this section of ATM1 deposition, it is not possible to determine accurately the exact length of the increasing δ

^{18}O value trend. It is thus unclear whether the onset of this increasing trend is linked to Younger Dryas forcings, but the possibility must be considered. Increasing carbon stable isotope values after the termination of the Younger Dryas could indicate an increase in the amount of CO_2 in the soil (Genty et al., 2001). Higher values indicate weaker soil development, perhaps due to drier conditions. Future work focusing on the Younger Dryas event recorded in ATM1 must include further dates within this segment of deposition. ATM1 contains calcite deposited prior to 10,300 bp and studies of Pleistocene paleoclimate in this region could be extended.

Northern latitude evidence of the Younger Dryas characterizes the event as cold and dry. However, the response in Central America seems to be cold but moist (Leyden 1995). Lacustrine and bog sediments in Guatemala and Costa Rica indicate a relatively moist Younger Dryas (Leyden 1995). The ATM1 record indicates that climate in Belize was moist during this period. Moist conditions may have been a result of increased seasonality (Berger 1991), which would have increased the strength of the Central American monsoon because of a southern shift in the Intertropical Convergence Zone (Curtis and Hodell 1993). If moist conditions recorded in ATM1 are a result of Younger Dryas forcings, ATM1 provides evidence for a connection between climate at high and low latitudes. The mechanism for the high/low latitude climate connection may be North Atlantic sea surface temperatures (SST). SST changes influence both trade winds and monsoon strength (Hughen 1996) and Licciardi (2009) suggests tropical Atlantic SST influence glacial fluctuations in southern Peru.

8.2 ka Event

Approximately 8,200 bp a global cold period (lasting 100-400 years depending on location) is recorded in several paleo-climatic archives all over the world (Lang et al., 2010; Hede et al, 2009; Hijma and Cohen, 2009). The draining of glacial lakes during the ultimate retreat of the Laurentide Ice Sheet caused the 8.2 ka event; due to the large influx of fresh water from the lake, thermohaline circulation in the Atlantic was disturbed and in turn caused a global climate event (Clark et al. 2004). This event has been recorded in multiple archives including: Greenland ice core records (GISP2), Cariaco basin sediment cores (Hughen et al., 1996), lacustrine sediment cores (Hodell et al. 1995), and another stalagmite in Central America (Lachinet et al. 2004) (Figure 9).

The ATM1 record displays a brief, pronounced high $\delta^{18}O$ excursion (0.51‰) around 8,500-8,625 bp (Figure 9). The Lachinet et al. (2004) data also shows a positive excursion in Costa Rican stalagmite calcite stable oxygen isotope values during the same time period. It must be noted that these conclusions from ATM1 are based on a linear age model with error bars larger than the duration of the excursion. Future studies must more accurately date the stalagmite in order to draw more precise conclusions. For this study, the implications of the linear age model presented here should be accepted with caution. The excursion associated with this event is the largest high excursion in the ATM1 isotope record. This indicates there was a ~100 year (or longer, according to the Venado Cave record) relatively dry period at this time. The 8.2 ka event is the most extreme abrupt climate change event on record for this time period, therefore it is likely that the event is responsible for the most pronounced excursion on the ATM1 oxygen stable isotope record from within this time period. Also, both ATM1 record and GISP2 data (Figure 10) show a sawtooth pattern directly before the excursion and a decline followed by a leveling off in the ~700 years following the excursion. Dating margin of error for ATM1 allows for the GISP1 and ATM1 events to be concurrent, limitations in the ATM1 age model also prevent determining whether there is a lead or lag relationship between this dry period in Belize and the global response to the Lake Agassiz draining,

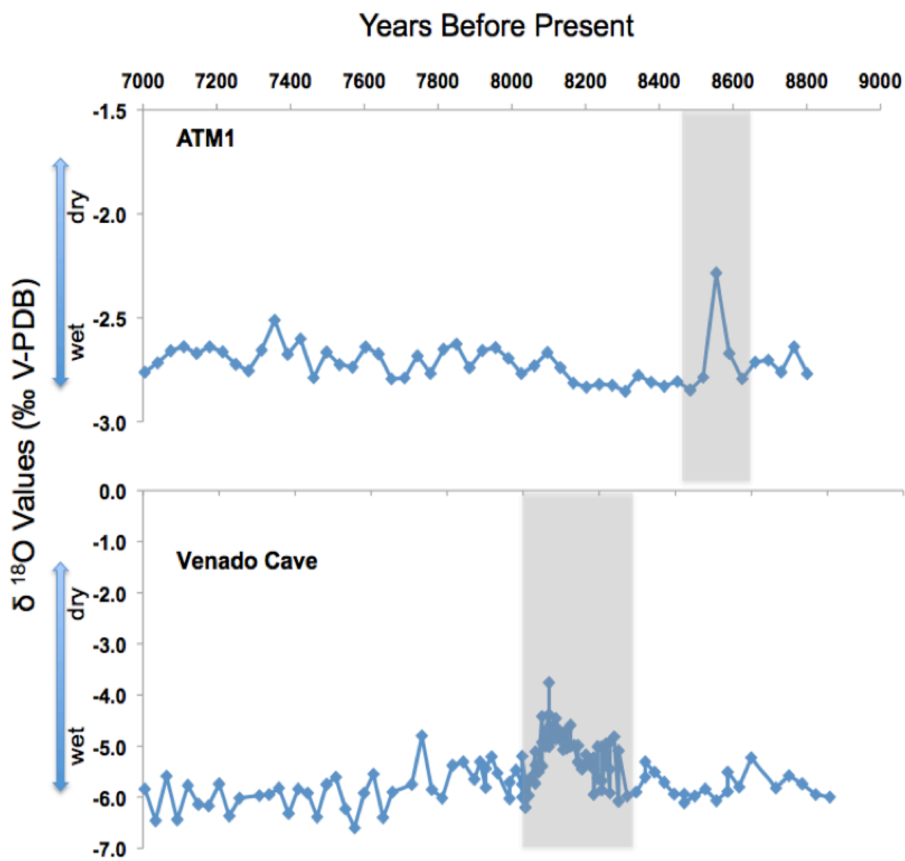

Figure 9. Comparison of ATM1 and Venado Cave stalagmite stable oxygen isotope ratios. Grey boxes highlight 8.2 ka abrupt climate event in each of the records.

but the timing and the magnitude of the excursion suggest the Belize climate event is associated with the globally recorded 8.2 ka event.

A weakening of the monsoon system may have caused dry conditions in Central America during the 8.2 ka event (Hastenrath, 1984). Two factors may have contributed to the weakening of the Central American Monsoon: a strengthening of the North

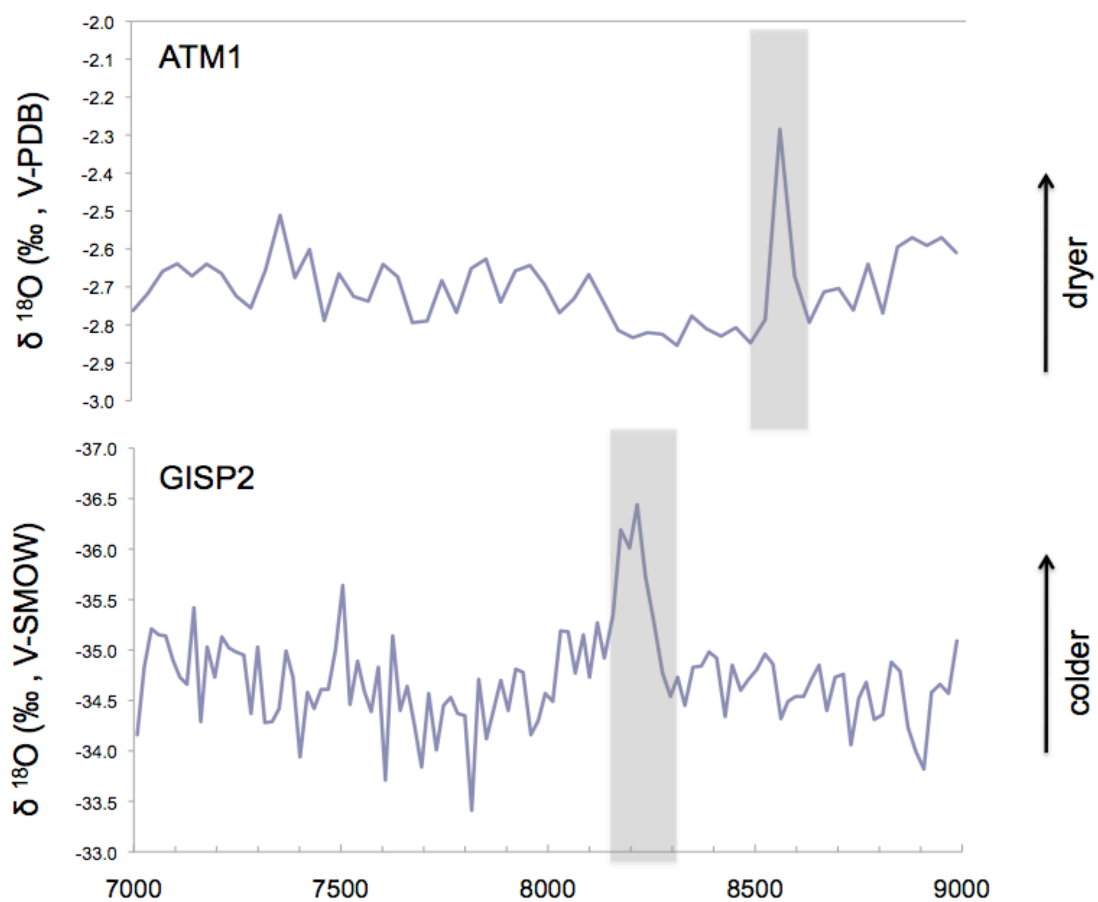

Figure 10. Oxygen isotope values from GISP2 ice core and ATM1 around 8000 bp. Grey areas highlight the 8.2 ka event in each of the records. ATM1 dating error bars allow for highlighted areas to match in time.

Atlantic anticyclone (also known as the Azores or Bermuda High), or a decrease in sea surface temperatures in the region. The North Atlantic anticyclone is a semi-permanent high-pressure system that lies at approximately 30 N in the eastern Atlantic (Hastenrath, 1984; Hughen et al., 1996). As a result of a strengthened North Atlantic anticyclone, the Intertropical Convergence zone would have shifted south (Giannini et al, 2000) and Central America would have experienced windy (Hughen et al, 1996) and dry conditions (Hastenrath, 1984) as a result. Cooler SST are also a possible cause for the 8.2 ka dry period because a decrease in SST delays the onset and hastens the end of the rainy season (Enfield and Alfaro 1999). If colder SST occurred in the tropical Atlantic, as they did in subtropical West Africa (deMenocal et al., 2000), then a shortened rainy season could have resulted in the increased oxygen stable isotope values observed during the 8.2 ka event. Dry conditions in the Belize region may have caused a reduction in wetland extent, and may have contributed to the decrease in methane amounts concurrent with the 8.2 ka event observed in the GISP2 ice core (Gischler, 2003).

6,000 bp Wet Event

Around 6,300 bp a large negative excursion (0.503 ‰) is observed in both carbon and oxygen stable isotope values. This negative excursion indicates a roughly 200 year relatively wet period followed by a recovery to previous Holocene averages. There are two possible explanations for this quick, pronounced period of high rainfall in central Belize.

The δ ^{18}O value negative excursion is concurrent with the Holocene transgression affecting the coast of Belize (Gischler 2003). The transgression along the central part of the coast lasted from 8,500-6,000 bp, raising sea levels starting in the south and moving northward (Gischler 2003). As sea level rose (Figure 11), atolls off the eastern coast were flooded creating restricted flow lagoons (Gischler 2003). These restricted flow lagoons may have acted as warm pools and increased evaporation off the coast of Belize. The increase in moisture availability may have created an increase in rainfall amounts in the vicinity of Actún Tunichil Muknal cave, and thus may have produced the low stable oxygen isotope excursion observed in the ATM1 record around 6,300 bp. The 6,300 bp excursion however is sharp and pronounced and it is proposed here that the increased rainfall amounts were only short-term because as sea level continued to rise, water circulation between the offshore lagoons and surrounding waters was restored (due to flooding of atolls) (Gischler 2003) and moisture availability returned to pre-transgression levels. The short-term restriction of lagoonal circulation may account for the observed period of increased rainfall in ATM1 around 6,300 bp. And a sudden shift to higher rainfall could alter carbon cycling and/or drip rate.

Another possible explanation for the 6,300 bp δ 18O value excursion is hurricane clusters. Clustered hurricane events have been observed in sedimentary cores from the coast of Belize (McColskey 2008). Two of these periods of increased hurricane activity, “clusters,” were dated to 4,450 bp and 5,450 bp and each lasted less than 1,000 years (McColskey 2008). Further constraint of the duration of these events was not possible in that study (McCloskey 2008). It is proposed here that the 6,300 bp low excursion in

ATM1 could be another hurricane cluster as seen in the sedimentary cores of McCloskey (2008) in central coastal Belize and Donnelly and Woodruff (2007) in Puerto Rico. Individual hurricanes recorded in stalagmites result in a sharp, low excursion in stable oxygen isotope values, but not in carbon stable isotope values, as seen in Frappier 2007 and it is expected that a period of increased hurricane activity would result in an extended low excursion over the span of the cluster. Because of this, it is concluded that a wetter

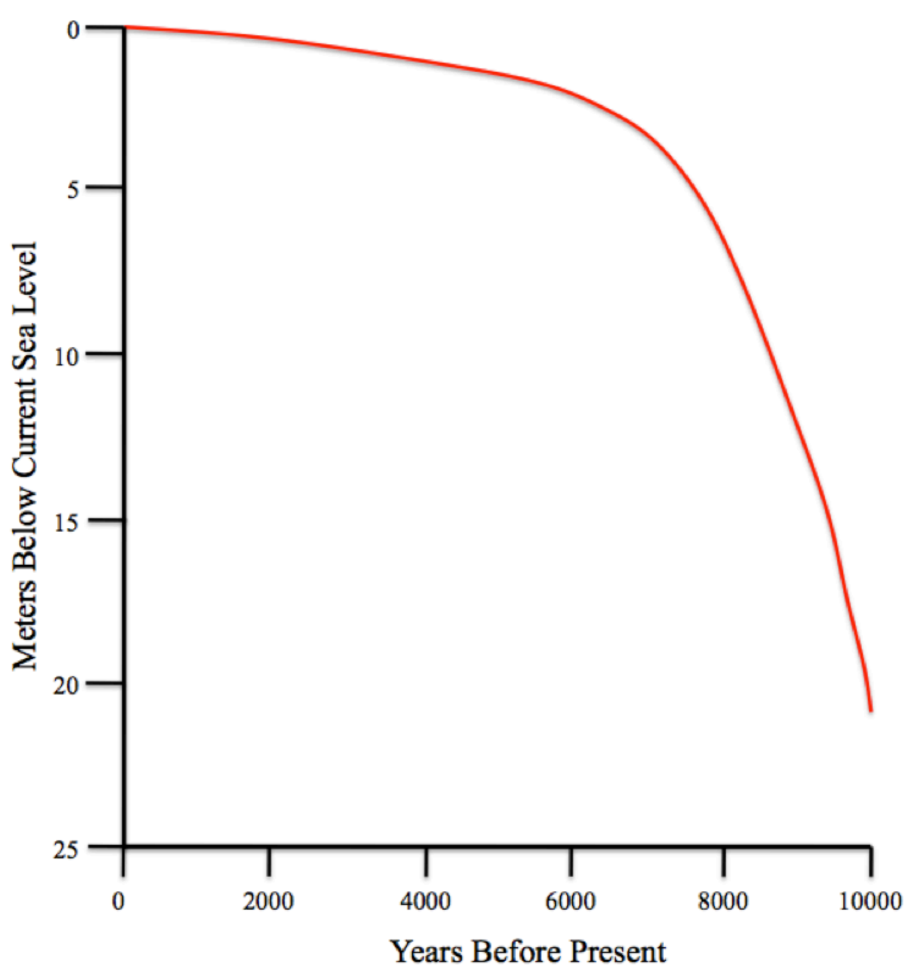

Figure 11. Belize sea level curve recreated using data from Gischler and Hudson (2004). Sea level rise off the coast of Belize supports the hypothesis of atoll lagoon restriction followed by total flooding of atoll creating a spike in rainfall amounts due to warm water creating more moisture available for regional rainfall.

climate is the more likely reason for the ATM1 stable oxygen isotope excursion at 6,300 bp.

Also supporting of this interpretation is the dual response of carbon and oxygen stable isotope values associated with the event. Hurricane events increase the hydraulic head in the epikarst system, because of increased infiltration due to an influx of water from the storm (Frappier 2002). This increases the drip rate feeding the stalagmite and in some cases is capable of altering the state of equilibrium deposition. This disequilibrium produces a decrease in the $\delta\ ^{13}C$ values of the stalagmite calcite because drip water $CO_{2(aq)}$ does not reach equilibrium with the cave atmosphere (Hendy 1971). This produces a low excursion in the $\delta\ ^{13}C$ values independent of and occurring before the low excursion in the $\delta\ ^{18}O$ values (Hendy 1971). The Frappier study focuses on individual storms, however it may be applied here because if an increased number of hurricanes increases drip rate over an extended period of time, disequilibrium deposition may persist for a longer period of time creating the dual response to hurricane water infiltration. The carbon and oxygen excursions in ATM1 are concurrent, but sampling resolution may mask a lead-lag relationship.

Oscillation of hurricane activity in the North Atlantic on a millennial scale as proposed by Liu and Fearn (2000) hypothesizes that movement of the Bermuda High induces periods of hurricane hyperactivity. Location of hurricane landfall is controlled by the location of the Bermuda High (Elsner et al 2000). If a hurricane cluster is responsible for the 6,300 bp excursion in ATM1, then this stalagmite record extends the record of the clustered hurricane events in Belize first proposed in McCloskey (2008), and also implies the Bermuda High control of hurricane landfall location goes as far back as ~6,300 bp.

Concluding Remarks

The ATM1 stalagmite stable isotope record presents a record of ITCZ-driven seasonal rainfall throughout the late Pleistocene to mid-Holocene. This 7,000-year record displays three major isotope excursions. Two of these are associated with well-documented global climate events, while the third is not.

The Younger Dryas, a 1,300-year cold period during the late Pleistocene manifests in tropical Belize (as recorded by ATM1) as a relatively moist period, and therefore a stronger monsoon dominated the seasonal rainfall regime. The 8.2 ka Event, a short cold period occurring ~8,200 bp, manifested itself in the opposite way as the Younger Dryas in central Belize. The 8.2 ka Event manifests as a cold, dry period at the study locale indicating a weaker monsoon dominating the region. The reasons for these opposite responses to global cooling are unknown, however it is possible that orbital forcings played a role in creating different relationships between the high and low latitude climates (Berger 1991).

A third major excursion in the ATM1 stable isotope record occurs around 6,300 bp. This relatively wet period lasting 200 years is not well documented in other global paleoclimate archives and as such it seems to be a more restricted regional scale phenomenon. Two possible explanations for this event are: eustatic seal level rise and hurricane clusters. Hurricane clusters are the favored hypothesis because of the dual response of both oxygen and carbon stable isotopes in the ATM1 record.

The ATM1 stable isotope record of three significant climate events in the tropics provides a valuable stepping-stone to uncovering the complex relationships between high and low latitude climate relationships.

Further research suggestions include additional dating samples to better constrain the ages of the stalagmite calcite and consequently better constrain the timing of major excursions in the stable isotope record. Additional accurate dates would also make the top section of stable isotope data useful in paleoclimatic interpretations. Analysis of older calcite from ATM1 (stratigraphically below the samples in this study) could provide paleoclimate information regarding the onset of the Younger Dryas; ATM1 may reveal additional useful paleoclimatic information if further research is conducted.

Works Cited

Alley, R.B. (1993) Abrupt accumulation increase at the Younger Dryas termination in the GISP2 ice core: Nature 362: 527–529.

Alley, R. B. (2000) The Younger Dryas cold interval as viewed from central Greenland *Quaternary Science Reviews* 19: 213–226.

Berger, A. and Loutre, M.F. (1991) Insolation values for the climate of the last 10 million years: *Quaternary Science Reviews* 10: 297-317.

Bradley, R. (1999) Paleoclimatology: Reconstructing Climates of the Quaternary: *International Geophysics Series* 68, Elsevier Academic Press, Burlington, MA.

Burns, S.J., Fleitmann, D., Matter, A., Neff, U., and Mangini, A. (2001) Speleothem evidence from Oman for continental pluvial events during interglacial periods: *Geology* 29: 623-626.

Cai, Y., Tan, L., Cheng, H., An, Z., Edwards, R.L., Kelly, M.J., Kong, X., Wang, X. (2010) The variation of summer monsoon precipitation in central China since the last deglaciation: *Earth and Planetary Science Letters* 291:21-31.

Clark, G.K.C., Leverington, D.W., Teller, J.T. & Dyke, A.S. (2004) Paleohydraulics of the last outburst flood from glacial Lake Agassiz and the 8200 BP cold event: *Quaternary Science Reviews* 23: 389–407.

Craig, H., (1957) Isotopic standards for carbon and oxygen and correction factors for mass-spectrometric analysis of carbon dioxide: *Geochemica et Cosmochimica Acta* 12:133-149.

Cruz, F.W., Burns, S.J., Karmann, I, Sharp, W. D., Vuille, M., Gerrari, J.A., (2006) A stalagmite record of changes in atmospheric circulation and soil processes in the Brazilian subtropics during the Late Pleistocene: *Quaternary Science Reviews* 25: 2749-2761.

Curtis, J.H. and Hodell, D.A. (1993) An isotopic and trace element study of ostracods from Lake Miragoane, Haiti: a 10,500 year record of paleosalinity and paleotmperature changes in the Caribbean: *Climate Change in Continental Isotopic Records*, 135-152.

Dansgaard W. (1964) Stable isotopes in precipitation. *Tellus* 16: 436 – 468.

deMenocal, P., Ortiz, J., Guilderson, T., and Sarnthein, M. (2000) Coherent high and low-latitude climate variability during the Holocene warm period: *Science* 288: 2198-2202.

Denniston, R.F., Gonzalez, L.A., Asmeron, Y., Polyak, V., Reagan, M.K., and Saltzman, M.R. (2001) A high-resolution speleothem record of climatic variability at the Allerod-Younger Dryas transition in Missouri, central United States: Palaeogeography, Palaeoclimatology, Palaeoecology 176: 147-155.

Donnely, J.P., and Woodruff, J.D. (2007) Intense hurricane activity over the past 5,000 years controlled by El Niño and the West African monsoon: *Nature* 447: 465-468.

Dorale, J., Edwards, R.L., Onac, B. P. (2002) Stable Isotopes as Environmental Indicators in Speleothems: Karst Processes and the Carbon Cycle: *Final Report of IGCP379*: 107-120.

Elsner, J.B., Liu, K.B., Kocher, B. (2000) Spatial variations in major US hurricane activity: statistics and a physical mechanism: *Journal of Climate* 13: 2293, 2305.

Enfield, D.B., and Alfaro, E.J. (1999) The dependence of Caribbean rainfall on the interaction of the tropical Atlantic and Pacific Oceans*: Journal of Climate* 12: 2093-2103.

Frappier, A. (2002) Master's Thesis: High-Resolution stable isotope dynamics recorded by speleothem calcite: New opportunities for paleotmpestology, paleometeorology and paleoecology: *University of New Hampshire.*

Frappier, A. (2006) Doctoral Dissertation: Recent extreme events in a tropical stalagmite: multi-proxy records and analysis of ecosystem $\delta^{13}C$ value sensitivity to weak climate forcing: *University of New Hampshire*.

Frappier, A., Sahagian, D., Carpenter, S.J., Gonzalez, L.A., Frappier, B.R. (2007) A stalagmite stable isotope record of recent tropical cyclone events: *Geology* 35: (2) 111-114.

Gascoyne, M. 1992, Palaeoclimate determination from cave calcite deposits. *Quaternary Science Reviews* 11: 609-632.

Genty, D., Baker, A., massault, M., Proctor, C., Gilmour, M., Pons-Branchu, E., Hamelin, B. (2001) Dead carbon in stalagmites: carbonate bedrock paleodissolution vs. ageing of soil organic matter. Implications for 13C variations in speleothems: *Geochimica et Cosmochimica Acta* 65: (20) 3443-3457

Giannini, A. Kushnir, Y and Ca, M.A. (2000) Interannual variability of Caribbean rainfall, ENSO and the Atlantic Ocean: *Journal of Climate* 13: 297-311.

Gischler, E., 2003, Holocene lagoonal development in the isolated carbonate platforms off Belize: *Sedimentary Geology* 159: 113-132.

Gischler, E., and Hudson, J.H. (2004) Holocene Development of Belize Barrier Reef: *Sedimentary Geology* 346: (3-4) 223-226.

Grootes, P.M., and Stuvier, M. (1997) Oxygen 18/16 variability in Greenland snow and ice with 10^3 to 10^5-year time resolution: *Journal of Geophysical Research* 102: 26455-26470.

Hastenrath, S. (1984) Interannual variability and annual cycle: Mechanisms of circulation and climate in the tropical Atlantic sector: *Monthly Weather Review* 112: 1097-1107.

Hede, M.U., Rasmussen, P., Noe-Nygaard, N., Clarke, A.L., Vinebrooke, R.D., and Olsen, J. (2010) Multiproxy evidence for terrestrial and aquatic ecosystem responses during the 8.2 ka cold event as recorded at Højby Sø, Denmark: *Quaternary Research* 73,3: 485-496.

Hijma, M.P., Cohen, K.M. (2009) Timing and magnitude of the sea level jump preluding the 8200 year event: *Geology* 38, 3: 275-278

Hendy, C.H. (1971) The isotopic geochemistry of speleothems, 1. The calculation of the effects of different modes of formation on the isotopic composition of speleothems and their applicability as paleoclimatic indicators: *Geochemica et Cosmochimica Acta* 35: 801-824.

Hodell, D.A., Curtis, J.H., and Brenner, M. (1995) Possible role of climate in collapse of the Classic Maya civilization: *Nature* 375: 391-394.

Hughen, K.A., Overpeck, J.T., Peterson, L.C., and Trumbore, S. (1996) Rapid climate changes in the tropical Atlantic region during the last declaciation: *Nature* 380: 51-54.

International Atomic Energy Agency.World Meteorological Organization (2009) Global network for isotopes in precipitation: *The GNIP database*, October 2009.

Kim, S.T., and O'Neil, J.R. (1997) Equilibrium and nonequilibrium oxygen isotope effects in synthetic carbonates: *Geochemica et Cosmochimica Acta* 61: 3461-3475.

Lachinet, M.S., Asmerom, Y., Burns, S.J., Patterson, W.P., Polyak, V.J., and Seltzer, G.O. (2004) Tropical response to the 8200 yr b.p. event? Speleothem isotopes indicate a weakened early Holocene monsoon in Costa Rica: *Geology* 32: (11) 957-960.

Lang, B., Bedford, A., Brooks, S.J., Jones, R.T., Richardson, N., Birks, H.J.B., and Marshall, J.D. (2010) Early-Holocene temperature variability inferred from chironomid assemblages at Hawes Water, northwest England: *The Holocene* 10.

Lauritzen, S.E., and Onac, B.P. (1999) Isotopic stratigraphy of a last interglacial stalagmite from northwestern Romania: Correlations with the deep-sea record and northern-latitude speleothem: *Journal of Cave and Karst Studies* 61: (1) 22-30.

Leyden, B.W. (1995) Evidence of the Younger Dryas in Central America, *Quaternary Science Reviews* 14: 833-839.

Liu, K.B., Fearn, M.L. (2000) Reconstruction of prehistoric landfall frequencies of catastrophic hurricanes in northwestern Florida from lake sediment records: *Quaternary Research* 54: 238-245.

McCloskey, T.A., and Keler, G. (2009) 5000 year sedimentary record of hurricane strikes on the central coast of Belize: *Quaternary International* 195: 53-68.

McDermott, F. (2004) Paleo-climate reconstruction from stable isotope variations in speleothems: a review: *Quaternary Science Reviews* 23: 901-918.

Nott, J. (2004) Paleotempestology- the study of pre-historic tropical cyclones- a review and implications for hazard assessment: *Environment International* 30: 433-447.

Richards, D.A., and Dorale, J.A. (2003) U-series chronology and environmental applications of speleothems: *Reviews in Mineralogy and Geochemistry* 52: 407-460.

Rozanski K, Araguas-Araguas L, Giofiantini R. (1993) Isotopic patterns in modern global precipitation: *Geophysical Monograph* 78: 1 – 36.

Shen, C., Edwards, R.L., Cheng, H., Dorale, J.A., Thomas, R.B., Moran, S.B., Weinstein, S.E. and Edmonds, H.N. (2002) Uranium and thorium isotopic and concentration measurements by magnetic sector inductively coupled plasma mass spectrometry: *Chemical Geology* 185: 165-178.

U.S. Geological Survey Names Committee (2007) Divisions of geologic time—Major chronostratigraphic and geochronologic units: *U.S. Geological Survey Fact Sheet 2007* 3015, 2 p.

Appendix A – Stable Isotope Notation

Delta notation (δ) is used to standardize stable isotope measurements. It is defined as follows:

$$\delta = \frac{(^{18}O/^{16}O)\text{ sample} - (^{18}O/^{16}O)\text{ standard}}{(^{18}O/^{16}O)\text{ standard}} \times 1000$$

where H is the ratio of heavy isotopes to light isotopes:

$$H = {}^{18}O/{}^{16}O \qquad \text{or} \qquad H = {}^{13}C/{}^{12}C$$

Carbonate samples use the global standard PDB (PeeDee Belemnite) from the PeeDee formation in South Carolina (Craig, 1957). V-PDB or Vienna-PeeDee Belemnite is now used as the global standard and is a correction for the PDB adopted in Vienna.

The units of the delta notation are parts per thousand (per mil / ‰). A sample with a larger proportion of the heavier isotope (^{18}O or ^{13}C) than the standard will have a positive δ value. A sample with a smaller fraction of the heavier isotope than the standard will have a negative δ value.

Appendix B – ATM1 Stable Isotope Data

Micromilled Stable Isotope Data – Study Period

Stable isotope values given in per mil (‰) and are measured as a deviation from the standard V-PDB. Age model spans 5,561 bp – 12,60m5 bp and present is taken as 2007, the year the radiometric dates were measured.

Depth in mm	Age Model (YBP)	$\delta^{13}C$ Value	$\delta\ ^{18}O$ Value
11.41	5561.00	-13.193	-3.411
11.43	5596.22	-13.251	-3.462
11.45	5631.44	-13.205	-3.394
11.47	5666.66	-13.254	-3.393
11.49	5701.88	-13.190	-3.371
11.51	5737.10	-13.183	-3.323
11.53	5772.32	-13.035	-3.027
11.55	5807.54	-12.978	-3.201
11.57	5842.76	-12.887	-3.059
11.59	5877.98	-12.940	-3.088
11.61	5913.20	-12.617	-2.990
11.63	5948.42	-12.655	-2.874
11.65	5983.64	-12.670	-2.998
11.67	6018.86	-12.591	-3.055
11.69	6054.08	-12.624	-3.010
11.71	6089.30	-12.429	-3.026
11.73	6124.52	-12.312	-2.872
11.75	6159.74	-12.375	-2.980
11.77	6194.96	-12.272	-2.781
11.79	6230.18	-12.201	-2.869
11.81	6265.40	-13.023	-3.211
11.83	6300.62	-12.250	-2.708
11.85	6335.84	-12.048	-3.079
11.87	6371.06	-11.994	-2.850
11.89	6406.28	-12.180	-2.868
11.91	6441.50	-12.207	-2.846
11.93	6476.72	-11.983	-2.852
11.95	6511.94	-11.890	-2.890
11.97	6547.16	-11.962	-2.915
11.99	6582.38	-11.887	-2.898
12.01	6617.60	-11.801	-2.894

12.03	6652.82	-11.824	-2.924
12.05	6688.04	-11.641	-2.669
12.09	6723.26	-11.566	-2.619
12.11	6758.48	-11.692	-2.806
12.13	6793.70	-11.514	-2.715
12.15	6828.92	-11.542	-2.711
12.17	6864.14	-11.624	-2.785
12.19	6899.36	-11.401	-2.688
12.21	6934.58	-11.412	-2.720
12.23	6969.80	-11.388	-2.824
12.25	7005.02	-11.370	-2.762
12.27	7040.24	-11.342	-2.717
12.29	7075.46	-11.208	-2.659
12.31	7110.68	-11.259	-2.639
12.33	7145.90	-11.074	-2.671
12.35	7181.12	-11.183	-2.640
12.37	7216.34	-11.137	-2.664
12.39	7251.56	-10.959	-2.724
12.41	7286.78	-10.954	-2.755
12.43	7322.00	-10.938	-2.656
12.45	7357.22	-10.870	-2.511
12.47	7392.44	-10.964	-2.676
12.49	7427.66	-10.920	-2.601
12.51	7462.88	-10.998	-2.789
12.53	7498.10	-10.973	-2.665
12.57	7533.32	-10.960	-2.725
12.59	7568.54	-10.905	-2.738
12.61	7603.76	-10.843	-2.640
12.63	7638.98	-10.916	-2.674
12.65	7674.20	-10.996	-2.794
12.67	7709.42	-10.964	-2.790
12.69	7744.64	-10.942	-2.683
12.71	7779.86	-10.934	-2.768
12.73	7815.08	-10.886	-2.651
12.75	7850.30	-10.871	-2.627
12.77	7885.52	-10.869	-2.740
12.79	7920.74	-10.990	-2.658
12.81	7955.96	-10.869	-2.643
12.83	7991.18	-10.889	-2.695
12.85	8026.40	-10.949	-2.768
12.87	8061.62	-10.889	-2.731
12.89	8096.84	-10.928	-2.667
12.91	8132.06	-10.860	-2.740
12.93	8167.28	-10.987	-2.814
12.95	8202.50	-10.929	-2.834

12.97	8237.72	-10.968	-2.820
12.99	8272.94	-10.928	-2.825
13.01	8308.16	-10.928	-2.854
13.03	8343.38	-10.960	-2.777
13.05	8378.60	-10.976	-2.810
13.07	8413.82	-10.949	-2.830
13.09	8449.04	-10.838	-2.807
13.11	8484.26	-10.850	-2.848
13.13	8519.48	-10.887	-2.786
13.15	8554.70	-10.753	-2.285
13.17	8589.92	-10.898	-2.671
13.19	8625.14	-10.869	-2.794
13.21	8660.36	-10.909	-2.713
13.25	8695.58	-10.816	-2.704
13.27	8730.80	-10.779	-2.761
13.29	8766.02	-10.517	-2.640
13.31	8801.24	-10.573	-2.769
13.33	8836.46	-10.405	-2.595
13.35	8871.68	-10.370	-2.570
13.37	8906.90	-10.343	-2.591
13.39	8942.12	-10.358	-2.570
13.41	8977.34	-10.249	-2.610
13.43	9012.56	-10.316	-2.736
13.45	9047.78	-10.153	-2.601
13.47	9083.00	-10.261	-2.876
13.49	9118.22	-10.184	-2.734
13.51	9153.44	-10.211	-2.786
13.53	9188.66	-10.115	-2.779
13.55	9223.88	-10.046	-2.673
13.57	9259.10	-9.962	-2.658
13.59	9294.32	-9.956	-2.638
13.61	9329.54	-10.048	-2.782
13.63	9364.76	-10.102	-2.856
13.65	9399.98	-9.921	-2.718
13.67	9435.20	-9.985	-2.706
13.69	9470.42	-9.968	-2.692
13.71	9505.64	-10.043	-2.754
13.73	9540.86	-10.131	-2.793
13.75	9576.08	-10.042	-2.786
13.77	9611.30	-10.076	-2.741
13.79	9646.52	-10.096	-2.686
13.81	9681.74	-10.176	-2.714
13.83	9716.96	-10.260	-2.767
13.85	9752.18	-10.357	-2.742
13.87	9787.40	-10.389	-2.757

13.89	9822.62	-10.496	-2.714
13.91	9857.84	-10.811	-2.791
13.93	9893.06	-10.760	-2.827
13.95	9928.28	-10.933	-2.831
13.97	9963.50	-10.875	-2.860
13.99	9998.72	-10.945	-2.891
14.01	10033.94	-11.070	-2.837
14.03	10069.16	-11.165	-2.925
14.05	10104.38	-11.054	-2.834
14.07	10139.60	-11.369	-3.019
14.09	10174.82	-11.434	-3.030
14.11	10210.04	-11.225	-2.940
14.13	10245.26	-11.132	-3.057
14.15	10280.48	-11.374	-2.987
14.19	10315.70	-11.626	-3.241
14.21	10350.92	-11.774	-3.388
14.23	10386.14	-11.760	-3.332
14.25	10421.36	-11.835	-3.367
14.27	10456.58	-11.995	-3.431
14.29	10491.80	-12.139	-3.438
14.31	10527.02	-12.204	-3.417
14.33	10562.24	-12.244	-3.453
14.35	10597.46	-12.369	-3.539
14.37	10632.68	-12.335	-3.495
14.39	10667.90	-12.518	-3.617
14.41	10703.12	-12.542	-3.550
14.43	10738.34	-12.567	-3.679
14.45	10773.56	-12.645	-3.615
14.47	10808.78	-12.641	-3.814
14.49	10844.00	-12.726	-3.661
14.53	10879.22	-12.647	-3.492
14.55	10914.44	-12.711	-3.727
14.57	10949.66	-12.736	-3.722
14.59	10984.88	-12.751	-3.710
14.61	11020.10	-12.859	-3.809
14.63	11055.32	-12.818	-3.799
14.65	11090.54	-12.929	-3.806
14.67	11125.76	-12.915	-3.839
14.69	11160.98	-13.019	-3.898
14.71	11196.20	-13.034	-3.964
14.73	11231.42	-13.032	-3.884
14.75	11266.64	-13.098	-4.024
14.77	11301.86	-13.158	-3.963
14.79	11337.08	-13.098	-3.948
14.83	11372.30	-13.155	-4.014

14.85	**11407.52**	**-13.207**	**-4.000**
14.87	**11442.74**	**-13.144**	**-3.994**
14.89	**11477.96**	**-13.171**	**-3.877**
14.91	**11513.18**	**-13.169**	**-3.901**
14.93	**11548.40**	**-13.188**	**-3.973**
14.95	**11583.62**	**-13.235**	**-3.980**
14.97	**11618.84**	**-13.132**	**-3.957**
14.99	**11654.06**	**-13.141**	**-3.914**
15.01	**11689.28**	**-13.186**	**-3.942**
15.03	**11724.50**	**-13.087**	**-4.061**
15.07	**11759.72**	**-13.141**	**-4.015**
15.09	**11794.94**	**-13.009**	**-3.955**
15.11	**11830.16**	**-13.064**	**-3.950**
15.13	**11865.38**	**-13.087**	**-3.998**
15.15	**11900.60**	**-13.075**	**-3.930**
15.17	**11935.82**	**-13.089**	**-4.004**
15.19	**11971.04**	**-13.105**	**-4.035**
15.21	**12006.26**	**-13.098**	**-4.003**
15.23	**12041.48**	**-13.150**	**-3.995**
15.27	**12076.70**	**-13.025**	**-4.180**
15.31	**12111.92**	**-13.078**	**-4.213**
15.33	**12147.14**	**-13.053**	**-4.173**
15.35	**12182.36**	**-13.132**	**-4.217**
15.39	**12217.58**	**-13.112**	**-4.225**
15.41	**12252.80**	**-13.106**	**-4.167**
15.43	**12288.02**	**-13.115**	**-4.147**
15.45	**12323.24**	**-13.126**	**-4.182**
15.47	**12358.46**	**-13.150**	**-4.235**
15.49	**12393.68**	**-13.145**	**-4.289**
15.51	**12428.90**	**-13.174**	**-4.252**
15.53	**12464.12**	**-13.143**	**-4.289**
15.55	**12499.34**	**-13.115**	**-4.232**
15.57	**12534.56**	**-13.166**	**-4.326**
15.59	**12569.78**	**-13.095**	**-4.267**
15.61	**12605.00**	**-13.176**	**-4.325**

Micromilled Stable Isotope Data – All Data

Depth in mm	$\delta^{13}C$ Values (‰)	$\delta\ ^{18}O$ Values (‰)
0.01	-8.733	-6.809
0.05	-8.483	-6.423
0.07	-7.940	-5.679
0.09	-7.633	-5.503
0.11	-7.673	-5.415
0.13	-7.576	-5.059
0.15	-7.811	-5.186
0.17	-8.184	-5.746
0.19	-7.827	-4.934
0.21	-7.897	-4.792
0.23	-7.817	-4.787
0.25	-7.644	-4.811
0.27	-8.168	-5.902
0.29	-7.815	-4.824
0.31	-7.846	-4.793
0.33	-7.772	-4.985
0.35	-7.888	-5.092
0.37	-7.772	-4.969
0.39	-7.842	-4.944
0.41	-7.889	-5.048
0.43	-8.023	-5.285
0.45	-7.973	-5.080
0.47	-8.145	-5.127
0.49	-8.104	-5.166
0.51	-8.048	-4.907
0.53	-8.139	-4.986
0.55	-8.149	-4.904
0.57	-8.297	-5.049
0.59	-8.334	-4.948
0.61	-8.415	-5.059
0.63	-8.354	-4.870
0.65	-8.346	-4.916
0.67	-8.467	-4.847
0.69	-8.606	-4.876
0.71	-8.669	-4.973
0.73	-8.651	-5.005
0.75	-8.623	-4.979
0.77	-8.790	-5.156

0.79	-8.391	-4.959
0.81	-8.060	-4.731
0.83	-8.050	-4.787
0.85	-7.917	-4.828
0.87	-7.939	-4.763
0.89	-7.575	-4.478
0.91	-7.857	-4.802
0.93	-7.884	-4.789
0.95	-7.806	-4.772
0.97	-7.755	-4.696
0.99	-7.832	-4.720
1.01	-7.835	-4.752
1.03	-7.898	-4.812
1.05	-7.834	-4.695
1.07	-7.914	-4.916
1.09	-8.021	-4.791
1.11	-8.046	-4.795
1.15	-8.324	-5.079
1.17	-8.270	-4.909
1.19	-8.491	-4.866
1.21	-8.819	-4.963
1.25	-9.060	-4.722
1.27	-9.220	-4.812
1.29	-9.388	-4.902
1.31	-9.563	-4.767
1.33	-9.682	-4.936
1.35	-9.830	-4.683
1.37	-9.841	-4.798
1.39	-10.099	-4.976
1.41	-10.071	-5.048
1.43	-9.935	-4.944
1.45	-10.079	-5.044
1.47	-10.030	-4.962
1.49	-9.893	-5.015
1.51	-9.775	-4.938
1.53	-9.955	-4.894
1.55	-9.714	-5.017
1.57	-9.556	-4.946
1.59	-9.602	-4.924
1.61	-9.674	-4.743
1.63	-10.154	-4.846
1.65	-10.632	-5.035
1.67	-11.079	-5.046
1.69	-11.238	-5.097
1.71	-11.535	-5.046

1.73	-11.801	-5.061
1.75	-12.085	-5.173
1.79	-11.003	-4.976
1.81	-11.477	-5.080
1.83	-12.005	-5.144
1.85	-12.146	-5.110
1.87	-12.233	-5.117
1.89	-12.183	-5.115
1.91	-12.181	-5.080
1.93	-12.163	-5.145
1.95	-12.051	-5.219
1.97	-12.166	-5.213
1.99	-12.097	-5.235
2.01	-10.983	-4.775
2.03	-11.527	-4.993
2.05	-12.055	-5.197
2.07	-12.059	-5.270
2.09	-11.883	-5.170
2.11	-11.964	-5.256
2.13	-11.921	-5.394
2.15	-12.043	-5.319
2.17	-11.814	-5.321
2.19	-11.818	-5.282
2.21	-11.766	-5.278
2.23	-11.866	-5.349
2.25	-11.852	-5.359
2.27	-11.883	-5.314
2.29	-12.011	-5.264
2.31	-12.187	-5.393
2.33	-12.185	-5.424
2.35	-12.359	-5.452
2.37	-12.327	-5.339
2.39	-12.380	-5.431
2.41	-12.496	-5.400
2.43	-12.605	-5.493
2.45	-12.581	-5.508
2.47	-12.622	-5.411
2.49	-12.580	-5.391
2.51	-12.721	-5.467
2.53	-12.677	-5.382
2.55	-12.687	-5.338
2.57	-12.728	-5.442
2.59	-12.686	-5.345
2.61	-12.739	-5.421
2.63	-12.730	-5.408

2.65	-12.714	-5.379
2.67	-12.862	-5.384
2.69	-12.800	-5.444
2.71	-12.827	-5.285
2.73	-12.786	-5.294
2.75	-12.930	-5.415
2.77	-12.619	-5.282
2.79	-12.949	-5.295
2.81	-12.709	-5.176
2.83	-12.657	-5.270
2.85	-12.770	-5.443
2.87	-12.567	-5.410
2.89	-12.664	-5.296
2.91	-12.689	-5.318
2.93	-12.582	-5.370
2.95	-12.602	-5.357
2.97	-12.508	-5.513
2.99	-12.616	-5.433
3.01	-12.531	-5.456
3.03	-12.287	-5.453
3.05	-12.417	-5.376
3.07	-12.430	-5.389
3.09	-12.517	-5.500
3.11	-12.484	-5.468
3.13	-12.402	-5.407
3.15	-12.352	-5.520
3.17	-12.209	-5.099
3.19	-12.394	-5.370
3.21	-12.456	-5.276
3.23	-12.430	-5.290
3.25	-12.447	-5.333
3.27	-12.529	-5.352
3.29	-12.453	-5.325
3.31	-12.493	-5.258
3.33	-12.501	-5.331
3.35	-12.562	-5.616
3.37	-12.536	-5.502
3.39	-12.429	-5.413
3.41	-12.477	-5.439
3.43	-12.526	-5.493
3.45	-12.485	-5.368
3.47	-12.548	-5.430
3.49	-12.549	-5.361
3.51	-12.633	-5.475
3.53	-12.500	-5.396

3.55	-12.516	-5.254
3.57	-12.524	-5.320
3.59	-12.593	-5.436
3.61	-12.537	-5.204
3.63	-12.606	-5.360
3.65	-12.578	-5.324
3.67	-12.629	-5.429
3.69	-12.625	-5.397
3.71	-12.589	-5.328
3.73	-12.571	-5.287
3.75	-12.628	-5.398
3.77	-12.622	-5.393
3.79	-12.659	-5.301
3.81	-12.555	-5.303
3.83	-12.469	-5.009
3.85	-12.564	-5.262
3.87	-12.639	-5.331
3.89	-12.604	-5.314
3.91	-12.546	-5.212
3.93	-12.498	-5.273
3.95	-12.567	-5.244
3.97	-12.547	-5.171
3.99	-12.626	-5.207
4.01	-12.592	-5.222
4.03	-11.447	-5.091
4.05	-12.528	-5.094
4.07	-12.651	-5.127
4.09	-12.625	-4.998
4.11	-12.708	-5.089
4.13	-12.695	-5.043
4.15	-12.764	-5.069
4.17	-12.765	-5.095
4.19	-12.882	-5.074
4.21	-12.628	-5.102
4.23	-12.841	-4.923
4.25	-12.770	-4.934
4.27	-12.902	-5.027
4.29	-12.870	-5.097
4.31	-12.937	-5.012
4.33	-13.042	-4.997
4.35	-13.019	-4.903
4.37	-13.032	-4.943
4.39	-13.026	-4.943
4.41	-13.038	-5.004
4.43	-13.012	-4.898

4.45	-13.023	-4.944
4.47	-13.026	-5.058
4.49	-12.982	-4.909
4.51	-13.031	-5.007
4.53	-13.012	-4.931
4.55	-13.032	-5.002
4.57	-12.893	-4.815
4.59	-12.981	-4.973
4.61	-12.828	-4.959
4.63	-12.983	-4.974
4.65	-12.918	-4.951
4.67	-12.947	-4.939
4.69	-12.917	-4.904
4.71	-12.951	-4.934
4.73	-12.915	-4.865
4.75	-12.944	-4.865
4.77	-12.943	-4.928
4.79	-12.975	-4.943
4.81	-12.921	-4.933
4.83	-12.981	-4.959
4.85	-12.960	-4.879
4.87	-12.939	-4.856
4.89	-12.942	-4.859
4.91	-12.992	-4.871
4.93	-12.977	-4.868
4.95	-13.164	-7.474
4.97	-13.043	-4.881
4.99	-13.094	-4.951
5.01	-13.073	-4.800
5.03	-13.087	-4.905
5.05	-13.091	-4.806
5.07	-13.139	-4.852
5.09	-13.150	-4.759
5.11	-13.213	-4.935
5.13	-13.351	-4.712
5.15	-13.325	-4.754
5.17	-13.396	-4.980
5.19	-13.326	-4.850
5.21	-13.487	-5.021
5.23	-13.317	-4.791
5.25	-13.404	-5.195
5.27	-13.301	-4.902
5.29	-13.282	-4.897
5.31	-13.258	-4.884
5.33	-13.363	-5.260

5.35	**-13.227**	**-4.952**
5.37	**-13.256**	**-5.223**
5.39	**-13.187**	**-4.980**
5.41	**-13.235**	**-5.008**
5.45	**-13.271**	**-5.116**
5.47	**-13.189**	**-4.853**
5.49	**-13.227**	**-4.836**
5.51	**-13.264**	**-4.846**
5.53	**-13.152**	**-4.788**
5.55	**-13.274**	**-4.758**
5.57	**-13.209**	**-4.803**
5.59	**-13.347**	**-4.910**
5.61	**-13.278**	**-4.694**
5.63	**-13.275**	**-4.728**
5.65	**-13.301**	**-4.766**
5.67	**-13.287**	**-4.676**
5.69	**-13.278**	**-4.657**
5.71	**-13.245**	**-4.570**
5.73	**-13.192**	**-4.508**
5.75	**-13.326**	**-4.732**
5.77	**-13.208**	**-4.547**
5.79	**-13.281**	**-4.710**
5.81	**-13.194**	**-4.574**
5.83	**-13.124**	**-4.630**
5.85	**-13.239**	**-4.744**
5.87	**-13.251**	**-4.700**
5.89	**-13.298**	**-4.926**
5.91	**-13.227**	**-4.624**
5.93	**-13.204**	**-4.835**
5.95	**-13.173**	**-4.803**
5.97	**-13.119**	**-4.716**
5.99	**-13.163**	**-4.887**
6.01	**-13.072**	**-4.560**
6.03	**-13.131**	**-4.647**
6.05	**-13.111**	**-4.663**
6.07	**-13.176**	**-4.736**
6.09	**-13.076**	**-4.612**
6.11	**-13.118**	**-4.648**
6.13	**-13.076**	**-4.594**
6.15	**-13.183**	**-4.757**
6.17	**-13.064**	**-4.559**
6.19	**-13.026**	**-4.497**
6.21	**-13.000**	**-4.500**
6.23	**-13.074**	**-4.547**
6.25	**-13.018**	**-4.507**

6.27	-13.016	-4.613
6.29	-12.942	-4.532
6.31	-12.936	-4.500
6.33	-12.979	-4.554
6.35	-12.906	-4.495
6.37	-12.812	-4.361
6.39	-12.875	-4.532
6.41	-12.879	-4.494
6.43	-12.911	-4.488
6.45	-12.913	-4.485
6.47	-12.955	-4.467
6.49	-12.809	-4.375
6.51	-12.992	-4.611
6.53	-12.978	-4.546
6.55	-13.167	-4.619
6.57	-13.003	-4.526
6.59	-13.096	-4.698
6.61	-13.074	-4.470
6.63	-13.069	-4.613
6.65	-13.047	-4.561
6.67	-13.088	-4.651
6.69	-12.904	-4.249
6.71	-13.223	-4.846
6.73	-12.975	-4.584
6.75	-13.045	-4.580
6.77	-12.962	-4.498
6.79	-12.963	-4.541
6.81	-13.053	-4.494
6.83	-13.007	-4.555
6.85	-13.035	-4.603
6.87	-13.119	-4.709
6.89	-13.202	-4.808
6.91	-13.057	-4.654
6.93	-13.164	-4.823
6.95	-13.156	-4.786
6.97	-13.079	-4.677
6.99	-13.162	-4.813
7.01	-13.045	-4.580
7.03	-13.253	-4.780
7.05	-13.262	-4.900
7.07	-13.236	-4.925
7.09	-13.045	-4.665
7.11	-13.265	-4.976
7.13	-13.272	-4.982
7.15	-13.485	-5.144

7.17	-13.242	-4.957
7.19	-13.256	-4.978
7.21	-13.276	-4.876
7.23	-13.206	-4.904
7.25	-13.287	-5.027
7.29	-13.324	-4.996
7.31	-13.061	-4.945
7.33	-13.277	-4.986
7.35	-13.225	-4.940
7.37	-13.279	-4.977
7.39	-13.198	-5.027
7.41	-13.106	-4.850
7.43	-13.087	-4.968
7.45	-13.085	-4.878
7.47	-13.051	-4.831
7.49	-13.041	-4.764
7.51	-12.999	-4.695
7.53	-13.036	-4.481
7.55	-13.026	-4.508
7.57	-13.065	-4.528
7.59	-13.001	-4.502
7.63	-12.976	-4.349
7.65	-13.017	-4.581
7.67	-12.977	-4.570
7.69	-12.935	-4.600
7.71	-12.896	-4.493
7.73	-12.925	-4.575
7.75	-12.900	-4.516
7.77	-12.914	-4.614
7.79	-12.753	-4.472
7.81	-12.704	-4.400
7.83	-12.795	-4.456
7.85	-12.754	-4.483
7.87	-12.916	-4.540
7.89	-12.851	-4.477
7.91	-12.881	-4.533
7.93	-12.901	-4.644
7.95	-12.872	-4.461
7.97	-12.951	-4.545
7.99	-12.940	-4.441
8.01	-12.931	-4.442
8.03	-12.823	-4.436
8.05	-12.897	-4.395
8.07	-12.855	-4.451
8.09	-12.831	-4.454

8.11	-12.842	-4.412
8.13	-12.834	-4.412
8.15	-12.848	-4.414
8.17	-12.772	-4.343
8.19	-12.857	-4.364
8.21	-12.768	-4.347
8.31	-12.749	-4.409
8.33	-12.624	-4.221
8.35	-12.589	-4.092
8.37	-12.701	-4.299
8.39	-12.688	-4.222
8.41	-12.590	-4.064
8.43	-12.565	-4.196
8.45	-12.583	-4.130
8.47	-12.607	-4.169
8.49	-12.634	-4.208
8.51	-12.704	-4.219
8.53	-12.651	-4.086
8.55	-12.641	-4.128
8.57	-12.711	-4.177
8.59	-12.746	-4.072
8.61	-12.740	-4.219
8.63	-12.831	-4.171
8.65	-12.755	-4.254
8.67	-12.841	-4.209
8.69	-12.826	-4.158
8.71	-12.910	-4.236
8.73	-12.820	-4.261
8.77	-12.867	-4.212
8.79	-12.928	-4.243
8.81	-12.888	-4.203
8.83	-12.962	-4.241
8.85	-12.882	-4.182
8.87	-12.911	-4.169
8.89	-12.946	-4.183
8.91	-12.983	-4.279
8.93	-13.022	-4.243
8.95	-13.005	-4.228
8.97	-13.020	-4.261
8.99	-13.057	-4.284
9.01	-13.060	-4.225
9.03	-13.122	-4.291
9.05	-13.057	-4.162
9.07	-13.198	-4.267
9.09	-13.130	-4.300

9.11	-13.213	-4.291
9.13	-13.280	-4.203
9.15	-13.240	-4.068
9.17	-13.276	-4.126
9.19	-13.298	-4.243
9.21	-13.308	-4.262
9.23	-13.239	-4.177
9.25	-13.154	-4.086
9.27	-13.266	-4.192
9.29	-13.285	-4.135
9.31	-13.263	-4.135
9.33	-13.254	-4.075
9.35	-13.208	-4.057
9.37	-13.214	-4.016
9.39	-13.246	-4.127
9.41	-13.299	-4.161
9.43	-13.261	-4.148
9.45	-13.273	-4.184
9.47	-13.241	-4.129
9.49	-13.261	-4.124
9.51	-13.272	-4.141
9.53	-13.286	-4.093
9.55	-13.297	-4.139
9.57	-13.316	-4.134
9.59	-13.311	-4.101
9.61	-13.286	-4.029
9.63	-13.325	-4.138
9.65	-13.338	-4.141
9.67	-13.328	-4.089
9.69	-13.334	-4.074
9.71	-13.317	-4.137
9.73	-13.298	-3.965
9.75	-13.328	-4.056
9.77	-13.284	-3.992
9.79	-13.294	-3.885
9.81	-13.390	-4.005
9.83	-13.394	-4.040
9.85	-13.401	-3.957
9.87	-13.276	-3.988
9.89	-13.408	-3.934
9.91	-13.415	-3.877
9.93	-13.444	-3.878
9.95	-13.358	-3.906
9.97	-13.468	-3.941
9.99	-13.406	-3.849

10.01	-13.416	-3.914
10.05	-13.309	-3.818
10.07	-13.438	-3.967
10.09	-13.474	-3.939
10.11	-13.416	-3.857
10.13	-13.356	-3.876
10.15	-13.343	-3.684
10.17	-13.378	-3.807
10.19	-13.431	-3.836
10.21	-13.348	-3.628
10.23	-13.396	-3.798
10.25	-13.373	-3.812
10.27	-13.346	-3.691
10.29	-13.380	-3.789
10.31	-13.396	-3.741
10.33	-13.438	-3.781
10.35	-13.429	-3.721
10.37	-13.390	-3.785
10.39	-13.337	-3.719
10.41	-13.386	-3.734
10.43	-13.410	-3.626
10.45	-13.378	-3.687
10.47	-13.328	-3.625
10.49	-13.320	-3.639
10.51	-13.247	-3.449
10.53	-13.336	-3.654
10.55	-13.407	-3.698
10.57	-13.381	-3.729
10.59	-13.269	-3.698
10.61	-13.374	-3.646
10.63	-13.338	-3.746
10.65	-13.312	-3.579
10.67	-13.374	-3.754
10.69	-13.326	-3.779
10.71	-13.296	-3.708
10.73	-13.297	-3.714
10.75	-13.254	-3.760
10.77	-13.264	-3.841
10.79	-13.280	-3.958
10.81	-13.166	-3.695
10.83	-13.217	-3.805
10.85	-13.162	-3.692
10.87	-13.222	-3.735
10.89	-13.252	-3.823
10.91	-13.294	-3.877

10.93	-13.199	-3.748
10.95	-13.181	-3.885
10.97	-13.138	-3.672
10.99	-13.251	-3.794
11.01	-13.080	-3.644
11.03	-13.185	-3.693
11.05	-13.240	-3.748
11.07	-13.192	-3.658
11.09	-13.226	-3.641
11.11	-13.186	-3.567
11.13	-13.223	-3.675
11.15	-13.239	-3.640
11.17	-13.196	-3.574
11.19	-13.197	-3.495
11.21	-13.206	-3.532
11.23	-13.192	-3.434
11.25	-13.192	-3.524
11.27	-13.244	-3.489
11.29	-13.246	-3.560
11.31	-13.263	-3.470
11.33	-13.175	-3.419
11.35	-13.252	-3.508
11.37	-13.237	-3.481
11.39	-13.305	-3.513
11.41	-13.193	-3.411
11.43	-13.251	-3.462
11.45	-13.205	-3.394
11.47	-13.254	-3.393
11.49	-13.190	-3.371
11.51	-13.183	-3.323
11.53	-13.035	-3.027
11.55	-12.978	-3.201
11.57	-12.887	-3.059
11.59	-12.940	-3.088
11.61	-12.617	-2.990
11.63	-12.655	-2.874
11.65	-12.670	-2.998
11.67	-12.591	-3.055
11.69	-12.624	-3.010
11.71	-12.429	-3.026
11.73	-12.312	-2.872
11.75	-12.375	-2.980
11.77	-12.272	-2.781
11.79	-12.201	-2.869
11.81	-13.023	-3.211

11.83	-12.250	-2.708
11.85	-12.048	-3.079
11.87	-11.994	-2.850
11.89	-12.180	-2.868
11.91	-12.207	-2.846
11.93	-11.983	-2.852
11.95	-11.890	-2.890
11.97	-11.962	-2.915
11.99	-11.887	-2.898
12.01	-11.801	-2.894
12.03	-11.824	-2.924
12.05	-11.641	-2.669
12.09	-11.566	-2.619
12.11	-11.692	-2.806
12.13	-11.514	-2.715
12.15	-11.542	-2.711
12.17	-11.624	-2.785
12.19	-11.401	-2.688
12.21	-11.412	-2.720
12.23	-11.388	-2.824
12.25	-11.370	-2.762
12.27	-11.342	-2.717
12.29	-11.208	-2.659
12.31	-11.259	-2.639
12.33	-11.074	-2.671
12.35	-11.183	-2.640
12.37	-11.137	-2.664
12.39	-10.959	-2.724
12.41	-10.954	-2.755
12.43	-10.938	-2.656
12.45	-10.870	-2.511
12.47	-10.964	-2.676
12.49	-10.920	-2.601
12.51	-10.998	-2.789
12.53	-10.973	-2.665
12.57	-10.960	-2.725
12.59	-10.905	-2.738
12.61	-10.843	-2.640
12.63	-10.916	-2.674
12.65	-10.996	-2.794
12.67	-10.964	-2.790
12.69	-10.942	-2.683
12.71	-10.934	-2.768
12.73	-10.886	-2.651
12.75	-10.871	-2.627

12.77	**-10.869**	**-2.740**
12.79	**-10.990**	**-2.658**
12.81	**-10.869**	**-2.643**
12.83	**-10.889**	**-2.695**
12.85	**-10.949**	**-2.768**
12.87	**-10.889**	**-2.731**
12.89	**-10.928**	**-2.667**
12.91	**-10.860**	**-2.740**
12.93	**-10.987**	**-2.814**
12.95	**-10.929**	**-2.834**
12.97	**-10.968**	**-2.820**
12.99	**-10.928**	**-2.825**
13.01	**-10.928**	**-2.854**
13.03	**-10.960**	**-2.777**
13.05	**-10.976**	**-2.810**
13.07	**-10.949**	**-2.830**
13.09	**-10.838**	**-2.807**
13.11	**-10.850**	**-2.848**
13.13	**-10.887**	**-2.786**
13.15	**-10.753**	**-2.285**
13.17	**-10.898**	**-2.671**
13.19	**-10.869**	**-2.794**
13.21	**-10.909**	**-2.713**
13.25	**-10.816**	**-2.704**
13.27	**-10.779**	**-2.761**
13.29	**-10.517**	**-2.640**
13.31	**-10.573**	**-2.769**
13.33	**-10.405**	**-2.595**
13.35	**-10.370**	**-2.570**
13.37	**-10.343**	**-2.591**
13.39	**-10.358**	**-2.570**
13.41	**-10.249**	**-2.610**
13.43	**-10.316**	**-2.736**
13.45	**-10.153**	**-2.601**
13.47	**-10.261**	**-2.876**
13.49	**-10.184**	**-2.734**
13.51	**-10.211**	**-2.786**
13.53	**-10.115**	**-2.779**
13.55	**-10.046**	**-2.673**
13.57	**-9.962**	**-2.658**
13.59	**-9.956**	**-2.638**
13.61	**-10.048**	**-2.782**
13.63	**-10.102**	**-2.856**
13.65	**-9.921**	**-2.718**
13.67	**-9.985**	**-2.706**

13.69	**-9.968**	**-2.692**
13.71	**-10.043**	**-2.754**
13.73	**-10.131**	**-2.793**
13.75	**-10.042**	**-2.786**
13.77	**-10.076**	**-2.741**
13.79	**-10.096**	**-2.686**
13.81	**-10.176**	**-2.714**
13.83	**-10.260**	**-2.767**
13.85	**-10.357**	**-2.742**
13.87	**-10.389**	**-2.757**
13.89	**-10.496**	**-2.714**
13.91	**-10.811**	**-2.791**
13.93	**-10.760**	**-2.827**
13.95	**-10.933**	**-2.831**
13.97	**-10.875**	**-2.860**
13.99	**-10.945**	**-2.891**
14.01	**-11.070**	**-2.837**
14.03	**-11.165**	**-2.925**
14.05	**-11.054**	**-2.834**
14.07	**-11.369**	**-3.019**
14.09	**-11.434**	**-3.030**
14.11	**-11.225**	**-2.940**
14.13	**-11.132**	**-3.057**
14.15	**-11.374**	**-2.987**
14.19	**-11.626**	**-3.241**
14.21	**-11.774**	**-3.388**
14.23	**-11.760**	**-3.332**
14.25	**-11.835**	**-3.367**
14.27	**-11.995**	**-3.431**
14.29	**-12.139**	**-3.438**
14.31	**-12.204**	**-3.417**
14.33	**-12.244**	**-3.453**
14.35	**-12.369**	**-3.539**
14.37	**-12.335**	**-3.495**
14.39	**-12.518**	**-3.617**
14.41	**-12.542**	**-3.550**
14.43	**-12.567**	**-3.679**
14.45	**-12.645**	**-3.615**
14.47	**-12.641**	**-3.814**
14.49	**-12.726**	**-3.661**
14.53	**-12.647**	**-3.492**
14.55	**-12.711**	**-3.727**
14.57	**-12.736**	**-3.722**
14.59	**-12.751**	**-3.710**
14.61	**-12.859**	**-3.809**

14.63	-12.818	-3.799
14.65	-12.929	-3.806
14.67	-12.915	-3.839
14.69	-13.019	-3.898
14.71	-13.034	-3.964
14.73	-13.032	-3.884
14.75	-13.098	-4.024
14.77	-13.158	-3.963
14.79	-13.098	-3.948
14.83	-13.155	-4.014
14.85	-13.207	-4.000
14.87	-13.144	-3.994
14.89	-13.171	-3.877
14.91	-13.169	-3.901
14.93	-13.188	-3.973
14.95	-13.235	-3.980
14.97	-13.132	-3.957
14.99	-13.141	-3.914
15.01	-13.186	-3.942
15.03	-13.087	-4.061
15.07	-13.141	-4.015
15.09	-13.009	-3.955
15.11	-13.064	-3.950
15.13	-13.087	-3.998
15.15	-13.075	-3.930
15.17	-13.089	-4.004
15.19	-13.105	-4.035
15.21	-13.098	-4.003
15.23	-13.150	-3.995
15.27	-13.025	-4.180
15.31	-13.078	-4.213
15.33	-13.053	-4.173
15.35	-13.132	-4.217
15.39	-13.112	-4.225
15.41	-13.106	-4.167
15.43	-13.115	-4.147
15.45	-13.126	-4.182
15.47	-13.150	-4.235
15.49	-13.145	-4.289
15.51	-13.174	-4.252
15.53	-13.143	-4.289
15.55	-13.115	-4.232
15.57	-13.166	-4.326
15.59	-13.095	-4.267
15.61	-13.176	-4.325

15.63	-13.137	-4.324
15.65	-13.184	-4.208
15.67	-13.181	-4.083
15.69	-13.111	-4.105
15.71	-13.105	-4.105
15.73	-13.144	-4.243
15.75	-13.172	-4.078
15.77	-13.144	-4.135
15.79	-13.119	-4.143
15.81	-13.113	-4.134
15.83	-13.035	-4.169
15.85	-13.057	-4.145
15.87	-13.120	-4.184
15.89	-12.953	-4.117
15.91	-13.084	-4.187
15.93	-12.929	-4.166
15.95	-13.010	-4.206
15.97	-12.945	-4.147
15.99	-13.034	-4.295
16.01	-12.861	-4.196
16.03	-13.075	-4.355
16.05	-12.654	-4.142
16.07	-12.832	-4.316
16.09	-12.750	-4.200
16.11	-12.991	-4.448
16.13	-12.678	-4.212
16.15	-12.787	-4.221
16.17	-12.523	-4.120
16.19	-12.789	-4.375
16.21	-12.574	-4.132
16.23	-12.570	-4.344
16.25	-12.546	-4.183
16.27	-12.482	-4.082
16.29	-12.526	-4.112
16.31	-12.730	-4.260
16.33	-12.558	-4.136
16.35	-12.732	-4.251
16.37	-12.525	-4.200
16.39	-12.772	-4.314
16.41	-12.541	-4.091
16.43	-12.684	-4.175
16.45	-12.071	-3.733
16.47	-12.266	-3.852
16.49	-12.068	-3.735
16.51	-12.007	-3.823

16.53	-12.000	-3.749
16.55	-12.041	-3.786
16.57	-12.069	-3.754
16.59	-12.171	-3.810
16.61	-12.022	-3.653
16.63	-12.074	-3.737
16.65	-12.096	-3.723
16.67	-12.118	-3.700
16.69	-12.163	-3.660
16.71	-12.174	-3.735
16.73	-12.187	-3.738
16.75	-12.275	-3.725
16.77	-12.350	-3.721
16.79	-12.263	-3.673
16.81	-12.321	-3.698
16.83	-12.331	-3.685
16.85	-12.376	-3.725
16.87	-12.335	-3.696
16.89	-12.452	-3.650
16.91	-12.396	-3.605
16.93	-12.453	-3.655
16.99	-12.439	-3.643
17.01	-12.521	-3.593
17.03	-12.488	-3.625
17.05	-12.554	-3.651
17.07	-12.591	-3.628
17.09	-12.556	-3.642
17.11	-12.560	-3.670
17.13	-12.534	-3.517
17.15	-12.618	-3.602
17.17	-12.556	-3.510
17.19	-12.511	-3.265
17.21	-12.897	-3.934
17.25	-12.615	-3.690
17.27	-12.399	-3.897
17.29	-12.633	-3.667
17.31	-12.694	-3.748
17.33	-12.679	-3.684
17.35	-12.700	-3.738
17.37	-12.676	-3.747
17.39	-12.699	-3.718
17.41	-12.652	-3.566
17.43	-12.663	-3.652
17.45	-12.664	-3.543
17.47	-12.657	-3.542

17.49	-12.624	-3.532
17.51	-12.607	-3.484
17.53	-12.756	-3.567
17.55	-12.753	-3.452
17.57	-12.592	-3.415
17.59	-12.668	-3.508
17.61	-12.658	-3.576
17.63	-12.664	-3.473
17.65	-12.626	-3.441
17.67	-12.672	-3.519
17.69	-12.588	-3.494
17.71	-12.616	-3.522
17.73	-12.591	-3.514
17.75	-12.611	-3.457
17.77	-12.556	-3.509
17.79	-12.661	-3.460
17.81	-12.596	-3.577
17.83	-12.804	-3.825
17.85	-12.617	-3.429
17.87	-12.671	-3.552
17.89	-12.681	-3.524
17.91	-12.708	-3.512
17.93	-12.751	-3.561
17.95	-12.717	-3.511
17.97	-12.770	-3.548
17.99	-12.753	-3.468
18.01	-12.754	-3.473
18.03	-12.748	-3.417
18.05	-12.721	-3.465
18.07	-12.772	-3.511
18.09	-12.720	-3.484
18.11	-12.710	-3.437
18.13	-12.744	-3.406
18.15	-12.734	-3.392
18.17	-12.724	-3.338
18.19	-12.710	-3.371
18.21	-12.714	-3.430
18.23	-12.749	-3.376
18.25	-12.745	-3.375
18.27	-12.720	-3.298
18.29	-12.729	-3.383
18.31	-12.716	-3.406
18.33	-12.717	-3.356
18.35	-12.729	-3.358
18.37	-12.731	-3.338

18.39	-12.756	-3.250
18.41	-12.820	-3.461
18.43	-12.696	-3.220
18.45	-12.714	-3.268
18.47	-12.705	-3.302
18.49	-12.626	-3.186
18.51	-12.714	-3.205
18.53	-12.661	-3.140
18.55	-12.717	-3.133
18.57	-12.656	-3.156
18.61	-12.712	-3.173
18.63	-12.661	-3.086
18.65	-12.710	-3.094
18.67	-12.656	-2.909
18.69	-12.660	-2.997
18.71	-12.671	-2.959
18.73	-12.647	-3.023
18.75	-12.616	-2.706
18.77	-12.554	-2.702
18.79	-12.703	-2.982
18.81	-12.675	-2.940
18.83	-12.706	-2.937
18.85	-12.750	-2.835
18.89	-12.785	-2.892
18.91	-12.770	-2.928
18.93	-12.789	-2.950
18.95	-12.683	-2.739
18.97	-12.761	-2.857
18.99	-12.741	-2.826
19.01	-12.732	-2.699
19.03	-12.652	-2.581
19.05	-12.701	-2.688
19.07	-12.689	-2.662
19.09	-12.660	-2.628
19.11	-12.641	-2.569
19.13	-12.581	-2.566
19.15	-12.642	-2.447
19.17	-12.628	-2.596
19.19	-12.426	-2.292
19.21	-12.388	-2.080
19.23	-12.416	-2.232
19.25	-12.340	-2.165
19.27	-12.241	-2.142
19.29	-12.191	-2.125
19.31	-12.136	-2.100

19.33	-12.150	-2.126
19.35	-12.012	-2.032
19.37	-11.918	-1.999
19.39	-11.758	-1.894
19.41	-11.610	-1.965
19.43	-11.531	-1.955
19.45	-11.614	-1.658
19.47	-11.477	-1.895
19.49	-11.246	-1.715
19.51	-11.111	-1.750
19.53	-11.063	-1.742
19.55	-10.926	-1.672
19.57	-10.835	-1.684
19.59	-10.683	-1.529
19.61	-10.626	-1.696
19.63	-10.497	-1.612
19.65	-10.343	-1.543
19.67	-10.349	-1.594
19.69	-10.180	-1.540
19.71	-10.082	-1.525
19.73	-10.193	-1.493
19.75	-10.081	-1.426
19.77	-10.494	-1.699
19.79	-10.226	-0.946
19.83	-10.461	-1.549
19.85	-10.768	-1.882
19.87	-10.696	-1.840
19.89	-10.733	-1.923
19.91	-10.739	-1.836
19.93	-10.615	-1.900
19.95	-10.708	-1.876
19.97	-10.707	-1.910
19.99	-10.577	-1.691
20.01	-10.561	-1.811
20.03	-10.505	-1.841
20.05	-10.389	-1.910
20.07	-10.316	-1.786
20.09	-10.222	-1.799
20.11	-10.381	-1.833
20.13	-10.136	-1.870
20.15	-10.280	-1.844
20.17	-10.056	-1.779
20.19	-9.999	-2.061
20.21	-9.803	-1.858
20.23	-9.866	-1.823

20.25	-9.817	-1.875
20.27	-9.869	-1.803
20.29	-9.820	-1.861
20.31	-9.843	-1.824
20.33	-9.911	-1.774
20.35	-9.862	-1.894
20.37	-10.040	-1.874
20.39	-10.055	-1.868
20.41	-10.174	-2.086
20.43	-10.189	-2.023
20.45	-10.244	-2.057
20.47	-10.140	-1.930
20.49	-10.170	-2.070
20.51	-10.199	-2.010
20.53	-10.136	-1.998
20.55	-10.016	-2.015
20.57	-9.932	-1.900
20.59	-9.933	-1.972
20.61	-9.851	-1.933
20.63	-9.826	-1.907
20.65	-9.817	-1.818
20.69	-9.685	-1.917
20.71	-9.545	-1.898
20.73	-9.471	-1.803
20.75	-9.499	-1.914
20.77	-9.472	-1.885
20.79	-9.437	-1.857
20.81	-9.286	-1.757
20.83	-9.279	-1.780
20.85	-9.187	-1.798
20.87	-9.128	-1.855
20.91	-8.976	-1.823
20.93	-9.064	-1.922
20.95	-8.881	-1.946
20.97	-8.868	-1.878
20.99	-8.721	-1.837
21.01	-8.729	-1.934
21.03	-8.525	-1.723
21.05	-8.733	-1.937
21.07	-8.445	-1.922
21.11	-8.259	-1.824
21.13	-8.183	-1.914
21.15	-7.971	-1.824
21.17	-8.050	-1.963
21.19	-8.091	-1.654

21.21	-8.064	-1.826
21.23	-8.047	-1.709
21.25	-8.155	-1.899
21.27	-8.124	-1.830
21.29	-8.078	-1.851
21.31	-8.115	-1.840
21.33	-8.249	-2.007
21.35	-8.170	-1.995
21.39	-7.875	-1.943
21.43	-8.117	-1.911
21.45	-7.815	-1.899
21.47	-8.021	-1.960
21.49	-8.509	-1.939
21.51	-8.317	-1.861
21.53	-8.574	-1.930
21.55	-8.737	-1.853
21.57	-9.016	-1.859
21.59	-9.189	-1.941
21.63	-9.404	-2.005
21.65	-9.624	-2.027
21.67	-9.731	-1.922
21.69	-9.917	-1.877
21.71	-9.821	-1.979
21.75	-9.941	-1.851
21.77	-9.922	-1.827
21.79	-10.104	-1.931
21.81	-10.096	-1.776
21.83	-10.203	-1.815
21.85	-10.128	-1.926
21.89	-10.191	-1.834
21.91	-10.140	-1.756
21.93	-10.221	-1.758
21.95	-10.080	-1.765
21.97	-10.170	-1.872
21.99	-10.145	-1.781
22.01	-10.147	-1.810
22.03	-10.090	-1.705
22.05	-10.072	-1.768
22.07	-10.133	-1.757
22.09	-10.045	-1.736
22.11	-9.922	-1.708
22.13	-9.610	-1.795
22.15	-9.706	-1.758
22.17	-9.564	-1.756
22.19	-9.448	-1.673

22.21	-9.415	-1.696
22.25	-9.087	-1.619
22.27	-9.048	-1.674
22.29	-8.839	-1.645
22.31	-8.871	-1.567
22.33	-8.888	-1.610
22.35	-8.941	-1.721
22.37	-8.797	-1.535
22.39	-8.668	-1.648
22.41	-8.613	-1.610
22.43	-8.659	-1.515
22.45	-8.536	-1.558
22.47	-8.522	-1.512
22.49	-8.225	-1.547
22.51	-8.255	-1.490
22.53	-8.163	-1.459
22.55	-7.989	-1.443
22.57	-8.085	-1.458
22.59	-7.956	-1.427
22.61	-7.941	-1.454
22.63	-8.022	-1.403
22.65	-7.833	-1.378
22.67	-8.032	-1.650
22.69	-8.084	-1.528
22.71	-7.947	-1.491
22.73	-8.090	-1.539
22.75	-8.009	-1.310
22.77	-8.239	-1.576
22.79	-8.288	-1.598
22.81	-8.456	-1.530
22.83	-8.638	-1.492
22.85	-8.658	-1.612
22.87	-8.883	-1.546
22.89	-8.966	-1.632
22.91	-9.091	-1.576
22.93	-10.045	-1.542
22.95	-10.362	-1.672
22.97	-10.208	-1.682
23.01	-9.705	-1.580
23.03	-9.530	-1.647
23.07	-8.769	-1.538
23.09	-8.458	-1.623
23.13	-7.729	-1.538
23.15	-7.503	-1.409
23.17	-7.417	-1.592

23.19	-7.415	-1.382
23.21	-7.406	-1.633
23.23	-7.391	-1.569
23.25	-7.325	-1.702
23.27	-7.304	-1.674
23.29	-7.339	-1.604
23.31	-7.344	-1.573
23.33	-7.277	-1.538
23.35	-7.205	-1.430
23.37	-7.272	-1.441
23.39	-7.144	-1.337
23.41	-7.219	-1.446
23.43	-7.154	-1.392
23.45	-7.140	-1.417
23.47	-6.962	-1.371
23.49	-7.002	-1.433
23.51	-6.912	-1.420
23.53	-6.945	-1.383
23.55	-6.798	-1.300
23.57	-6.827	-1.236
23.59	-6.754	-1.263
23.61	-6.748	-1.350
23.63	-6.614	-1.272
23.65	-6.628	-1.177
23.67	-6.630	-1.199
23.69	-6.761	-1.392
23.71	-6.752	-1.301
23.73	-6.803	-1.376
23.75	-6.775	-1.511
23.77	-6.764	-1.432
23.79	-6.718	-1.448
23.81	-6.745	-1.471
23.83	-6.702	-1.521
23.85	-6.832	-1.528
23.87	-6.765	-1.488
23.89	-6.776	-1.480
23.91	-6.633	-1.312
23.93	-6.728	-1.508
23.95	-6.684	-1.225
23.97	-6.844	-1.508
23.99	-6.781	-1.310
24.01	-6.796	-1.336
24.03	-6.800	-1.498
24.05	-6.822	-1.399
24.07	-6.859	-1.406

24.09	-6.881	-1.410
24.11	-6.991	-1.619
24.13	-6.951	-1.598
24.17	-7.135	-1.583
24.19	-7.181	-1.484
24.21	-7.330	-1.633
24.23	-7.334	-1.635
24.25	-7.252	-1.578
24.27	-7.359	-1.654
24.29	-7.447	-1.726
24.31	-7.471	-1.598
24.33	-7.493	-1.704
24.35	-7.569	-1.771
24.37	-7.677	-1.890
24.39	-7.566	-1.875
24.43	-7.733	-1.987
24.45	-7.780	-1.984
24.47	-7.359	-1.839
24.49	-7.550	-1.926
24.53	-7.011	-1.895
24.55	-6.959	-1.948
24.57	-6.829	-1.835
24.59	-7.433	-1.969
24.61	-7.075	-1.870
24.63	-6.839	-1.962
24.65	-6.593	-1.899
24.67	-6.616	-1.898
24.69	-6.551	-1.922
24.71	-6.503	-1.888
24.73	-6.497	-1.864
24.77	-6.432	-1.914
24.79	-6.493	-1.960
24.83	-6.431	-1.827
24.85	-6.318	-1.854
24.87	-6.440	-1.933
24.89	-6.455	-1.950
24.91	-6.582	-2.080
24.93	-6.372	-1.909
24.95	-6.246	-1.845
24.97	-6.286	-1.861
24.99	-6.207	-1.892
25.01	-6.118	-1.811
25.03	-6.187	-1.810
25.05	-6.286	-1.971
25.07	-6.044	-1.808

25.09	-6.126	-1.937
25.11	-5.906	-1.760
25.13	-5.834	-1.721
25.15	-5.670	-1.689
25.19	-5.726	-1.739
25.21	-5.549	-1.530
25.23	-5.481	-1.495
25.25	-5.535	-1.632
25.27	-5.626	-1.726
25.29	-5.681	-1.487
25.31	-5.564	-1.421
25.33	-5.509	-1.336
25.35	-5.574	-1.550
25.37	-5.569	-1.557
25.41	-5.415	-1.439
25.43	-5.427	-1.605
25.45	-5.358	-1.464
25.47	-5.323	-1.653
25.51	-5.303	-1.569
25.53	-5.254	-1.448
25.55	-5.184	-1.498
25.57	-5.141	-1.467
25.61	-5.198	-1.526
25.63	-5.080	-1.426
25.65	-5.123	-1.544
25.67	-5.070	-1.473
25.69	-5.030	-1.576
25.71	-5.058	-1.515
25.73	-4.985	-1.418
25.75	-5.052	-1.522
25.77	-5.086	-1.582
25.79	-5.043	-1.552
25.81	-5.097	-1.451
25.83	-5.090	-1.594
25.85	-5.296	-2.040
25.87	-5.256	-1.655
25.89	-5.352	-1.672
25.91	-5.277	-1.506
25.93	-5.425	-1.625
25.95	-5.394	-1.678
25.97	-5.436	-1.586
25.99	-5.436	-1.501
26.01	-5.466	-1.530
26.03	-5.519	-1.680
26.05	-5.558	-1.519

26.07	**-5.549**	**-1.592**
26.09	**-6.463**	**-3.316**
26.11	**-6.535**	**-2.149**
26.13	**-6.701**	**-2.153**
26.15	**-6.700**	**-2.181**
26.17	**-6.824**	**-2.218**
26.21	**-7.167**	**-2.351**
26.27	**-7.309**	**-2.297**
26.29	**-7.179**	**-2.070**
26.31	**-7.348**	**-2.110**
26.33	**-7.466**	**-2.131**
26.35	**-7.416**	**-2.187**
26.37	**-7.484**	**-2.143**

<u>Hendy Test Stable Isotope Data</u>

Distence from Apex (mm)	**Depth from top of ATM1 (cm)**	**$\delta^{13}C$ (‰)**	**$\delta\ ^{18}O$ (‰)**
<u>Hendy 1</u>			
6.4	**1.6430**	**-12.906**	**-4.359**
4.1	**1.6430**	**-12.374**	**-4.058**
0	**1.6430**	**-12.684**	**-4.175**
<u>Hendy 2</u>			
9.3	**2.4470**	**-7.278**	**-1.988**
7.2	**2.4470**	**-7.561**	**-1.964**
0	**2.4470**	**-7.359**	**-1.839**